Evaluation of Atmospheric Pressure Loading Effects on GPS-based Positioning

HERMAN ANDERSSON

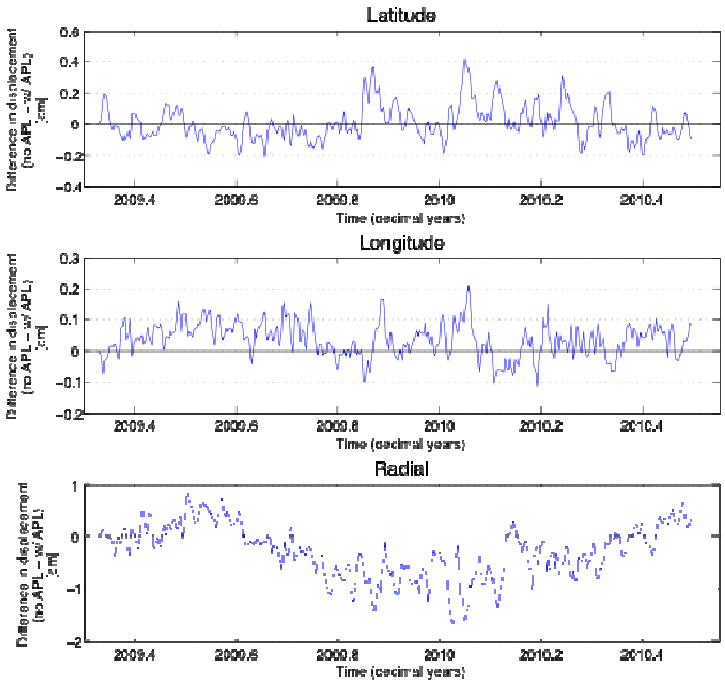

Examiner: Hans-Georg Scherneck, Chalmers University of Technology

Supervisors: Frank H. Webb, Jet Propulsion Laboratory
Jan M. Johansson, Chalmers University of Technology

Department of Earth and Space Science
CHALMERS UNIVERSITY OF TECHNOLOGY
Göteborg, Sweden 2010

Evaluation of Atmospheric Pressure Loading Effects on GPS-based Positioning

HERMAN ANDERSSON, 2010

Department of Radio and Space Science
Chalmers University of Technology
SE-412 96 Göteborg
Sweden

Cover:

Differences in displacement time series at Bishkek (POL2) with and without applying the model for atmospheric pressure loading

Chalmers University of Technology
Göteborg, Sweden

ABSTRACT

As atmospheric pressure varies over time it exerts a dynamic load on the Earth, causing crustal deformations. When performing high precision GPS measurements, such deformations may affect the accuracy of the measurements. This Master of Science thesis aims at describing how atmospheric pressure loading tends to affect precise point positioning with GPS measurements and evaluate the effects. Furthermore, the goal of the long-term work, of which this evaluation is part, is to implement correction terms for crustal movements derived from atmospheric pressure loading in the GPS data processing software package GIPSY-OASIS and to perform tests to investigate the results on precise positioning.

Deformation time-series data, based on 6-hourly NCEP reanalysis pressure data in a 2.5° x 2.5° grid, is downloaded from a database administrated by the VLBI group at NASA Goddard Space Flight Center. Subsequently, the deformation data is applied on GPS measurement data as daily average values and the results are analyzed.

Results from comparing GPS displacement time series data with and without having applied the model for atmospheric pressure loading, respectively, show a reduced daily scatter at most of the investigated sites, especially for the radial component, after implementation of the model. This suggests that implementing terms of atmospheric pressure loading can enhance the accuracy in GPS measurements.

Keywords:

Atmospheric pressure loading, crustal deformation, Global Positioning System (GPS), GPS-Inferred Positioning System – Orbit Analysis Simulation Software (GIPSY-OASIS), GPS site, time-series, pressure grid

ACKNOWLEDGEMENTS

This Master of Science thesis project has been made possible with help and support from many people, at Jet Propulsion Laboratory in Pasadena, California as well as at Chalmers University of Technology in Göteborg, Sweden, and also my family.

I would especially like to express my gratitude to the following people:

Hans-Georg Scherneck, my examiner at Chalmers University of Technology, for preparing me for my visit to JPL and sharing his wisdom in the field of atmospheric loading.

Jan Johansson, my supervisor at Chalmers University of Technology, for giving me the opportunity to go to JPL, preparing me for my visit and always being helpful, both with issues directly concerning the project and of more general nature.

Frank Webb, my supervisor at JPL, for giving me the opportunity to come to JPL and providing important guidance throughout the project.

Shailen Desai, for giving me supportive guidance and important input to my work during my visit at JPL.

Angelyn "Angie" Moore, for always being there to answer my numerous questions concerning everything included in the project and showing patience with my limitations in programming skills.

Allyson Beatrice, for helping me prepare everything for my visit to JPL and taking care of everything not directly associated with my project while in Pasadena so I could focus entirely on my work.

Rob DeCarvalho, my officemate at JPL, for helping me solving all kinds of problems, big and small, that I encountered in my work, and for all the interesting discussions during lunches.

Last but not least I would like to thank my wonderful girlfriend Elin for joining me in California and planning the weekends for us to explore "the Golden State", and for always being a great support.

TABLE OF CONTENTS

APPENDIX

1. INTRODUCTION

In everyday life people are likely to encounter Global Navigation Satellite Systems (GNSS) such as the American Global Positioning System (GPS), which has numerous widespread applications. Geophysics, weather forecasting, navigation and construction are just a few of the fields in which GPS technique is used. In 1973 the U.S. Department of Defense started developing GPS and since then there is an ongoing process to improve the system (U.S. National Executive Committee for Space-Based Positioning, Navigation and Timing, 2009).

As the use of GPS is increasing, so is the demand of the system's precision and accuracy. Over the last decade the progress of decreasing error sources affecting the system has taken a large step forward with advances in receiver hardware and data analysis software. However, the system is not yet perfect. One of the remaining error sources in GPS is associated with crustal movements of the Earth due to atmospheric pressure loading.

The atmosphere exerts a pressure on the Earth's crust causing elastic deformation of the solid Earth and thus movements on the ground surface. The effects of this dynamic load, notably referred to as atmospheric pressure loading, tend to vary with time as the atmospheric mass distribution changes globally. The magnitude of the effects fluctuates with time as the pressure varies, but also depending on location. Oceans tend to reduce the effects of the atmospheric pressure since large amounts of water can relocate and thereby absorb the loading. However, the effect is still present in shallow waters. The amplitude of the caused displacements has proven to be as large as 2 cm in the vertical direction and 3 mm horizontally (Petrov & Boy, 2004), or comprise up to 24 % of the total variance in vertical component estimates (van Dam, Blewitt, & Heflin, 1994) and is thus of importance when computing satellite orbit data. The Global Positioning System (GPS), which is based on such data, can be refined by implementing correction terms for ground surface movements derived from atmospheric pressure loading in GPS data processing software such as GIPSY-OASIS, a software package developed by the National Aeronautics and Space Administration (NASA) at Jet Propulsion Laboratory (JPL) in Pasadena, California.

This Master of Science thesis aims at describing influences from atmospheric pressure loading in connection to GPS measurement data and how atmospheric pressure loading can affect such measurements. Moreover, the project is part of an on-going work on implementing correction terms for atmospheric pressure loading in GIPSY-OASIS. The model is to comprise meteorological data collected at weather forecasting centers such as the National Centers for Environmental Prediction (NCEP).

2. BACKGROUND

This chapter contains descriptions of techniques and technologies essential for carrying out this project. A summary of how the Global Positioning System (GPS) works is included, as is a description of the GIPSY-OASIS software as well as an overview of the meteorological data used.

2.1. GLOBAL POSITIONING SYSTEM

The Global Positioning System, GPS, was initially an American military system for navigational purposes. Originally denoted NAVSTAR (Navigation Satellite Time And Ranging) GPS has been under development ever since the start in 1973 at the United States Department of Defense (Wells, et al., 1986). Today the system, which is still owned by the U.S. government, provides various positioning, navigation and timing (PNT) services not only for military purposes but also for civilians to use globally. As displayed in Figure 1 below, GPS is based on interaction between three different segments, namely the space segment, the control segment and the user/receiver segment (U.S. National Executive Committee for Space-Based Positioning, Navigation and Timing, 2009). Below, these three segments and their principles are described.

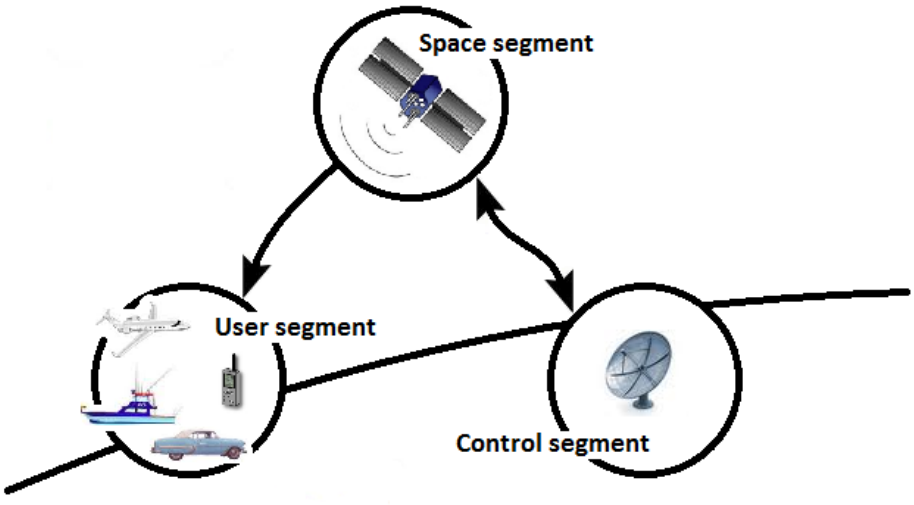

FIGURE 1. GPS IS BASED ON INTERACTION BETWEEN THREE DIFFERENT SEGMENTS

2.1.1. SPACE SEGMENT

The space segment consists of 32 (originally 24) satellites orbiting in six nearly circular orbit planes, inclined 55°. The satellites, operating at a nominal altitude of 20,180 km with a period of 11 hours and 58 minutes, carry atomic clocks and continuously transmit unique messages with information about their position and state, including orbit data and clock parameters. Moreover, signals are broadcast via two L-band carrier frequencies; L_1 (1575.42 MHz) and L_2 (1227.60 MHz) respectively. The L_1 carrier is modulated by a military precision "P-code" at 10.23 MHz along with a civilian course acquisition "C/A-code" whilst the L_2 carrier is modulated only by the P-code. (Wells, et al., 1986)

2.1.2. CONTROL SEGMENT

In order to calibrate satellite orbits and upload navigational information to the satellites, a global control segment is structurally organized. Presently there are five monitoring ground stations, so called reference frame sites, estimating orbit information from pseudorange observations. They are situated in Kwajalein Atoll (1), Colorado Springs (2), Diego Garcia Island (3), Honolulu (4) and Ascension Island (5) as displayed in Figure 2 below.

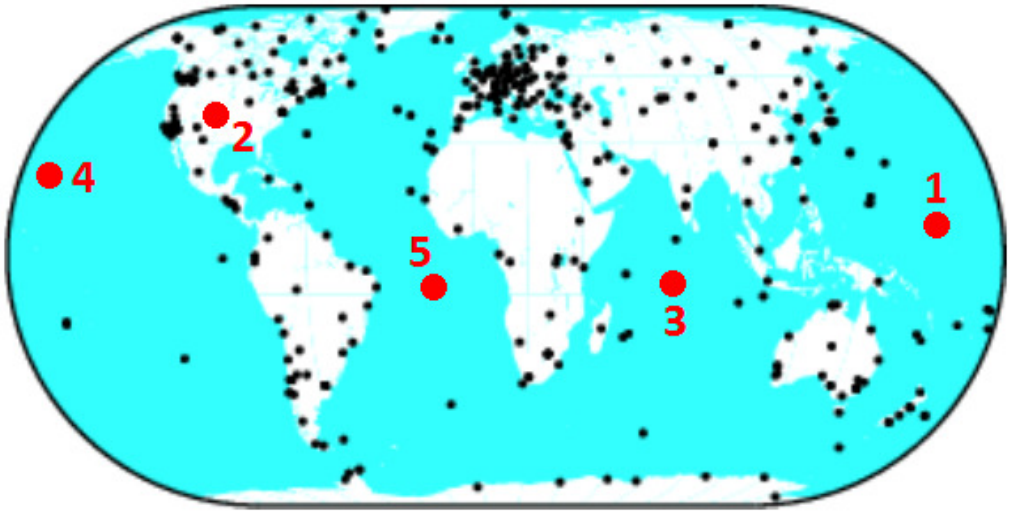

FIGURE 2. THE IGS TRACKING NETWORK WITH REFERENCE FRAME SITES HIGHLIGHTED IN RED

The five reference frame sites belong to the IGS (**I**nternational **G**NSS **S**ervice) tracking network consisting of numerous GPS stations spread all over the world, tracking both code and phase data from at least eight visible satellites simultaneously. Such stations can be operated and controlled by practically anyone who can meet the requirements of the IGS Site Guidelines established at the IGS Central Bureau (IGS Central Bureau, 2007). The IGS Site Guidelines include requirements on submitting tracking data, meteorological data and timing activities amongst others. For each included field there are some equipment and operational characteristics that are "strictly required" and some that are "additionally desired", meaning that the features of the different stations in the IGS tracking network vary, which may need to be taken into consideration when using the tracking stations for analysis.

2.1.3. USER/RECEIVER SEGMENT

The third segment needed in GPS measurement is the user/receiver segment. This is where the signals sent out from the satellites in the space segment are acquired and interpreted. The basic idea behind this step is to measure the difference between the time a message is sent from a satellite and the time it is collected by a receiver, and then calculate the distance according to

equation 1 below. The distance between a satellite and a receiver is usually denoted pseudorange.

$$R = c \cdot (t_r - t_{sat}) \quad (1)$$ where,

R is the pseudorange,
c is the speed of light,
t_r is the time when the signal reaches the receiver and
t_{sat} is the time when the signal is sent from the satellite.

As modern receivers have parallel working channels, it is possible to acquire several satellites simultaneously. As mentioned earlier, all satellites transmit unique code sequences and thus the receivers are able to separate the different satellites from one another. Accordingly, receivers can determine their position from knowledge of the distances to multiple satellites.

There is, however, a more precise alternative to this traditional method of code based positioning using the carrier phase instead. By measuring the phase difference between the generated and the received code, millimeter precision can be obtained. This more precise method is used in this project. Regardless of which method is used, receivers commonly consist of three main components; an antenna, a receiver-processor unit and a control/display.

In general, the accuracy of GPS positioning depends on the geometric constellation of the satellites used and the precision of a single pseudorange is commonly expressed by the standard deviation, σ_r. When describing the associated error in position, the term Dilution Of Precision, DOP, is introduced. As the accuracy is depending on satellite orbit constellation the DOP is not the same in all directions, north, east and vertical, and applies also on time measurements. (Seeber, 1993)

2.2. GIPSY-OASIS

GPS data can be collected and processed by using the software package GIPSY-OASIS, which consists of two parts with common modules. The first part,

GIPSY, short for GPS-Inferred Positioning System, is intended for standard geodetic applications while the second part, OASIS (Orbit Analysis Simulation Software), is a software package for analysis of orbit data covariance. JPL started developing the software in 1985 and it has developed and improved ever since. The current version of GIPSY-OASIS runs on the UNIX operating system and can be used for processing not only GPS data but also SLR (Satellite Laser Ranging), TOPEX (TOPography Experiment) and DORIS (Doppler Orbitography and Radio positioning Integrated by Satellite) observations. (Gregorius, 1996)

2.2.1. SOFTWARE OVERVIEW

A flowchart thoroughly displaying the outline of the traditional GIPSY-OASIS software is enclosed in appendix A. The flowchart shows the main components of the software package and the two main input branches, namely obervational data and orbit data. The chart in Figure 3 below shows an overview of what steps are included in a typical GIPSY-OASIS data flow.

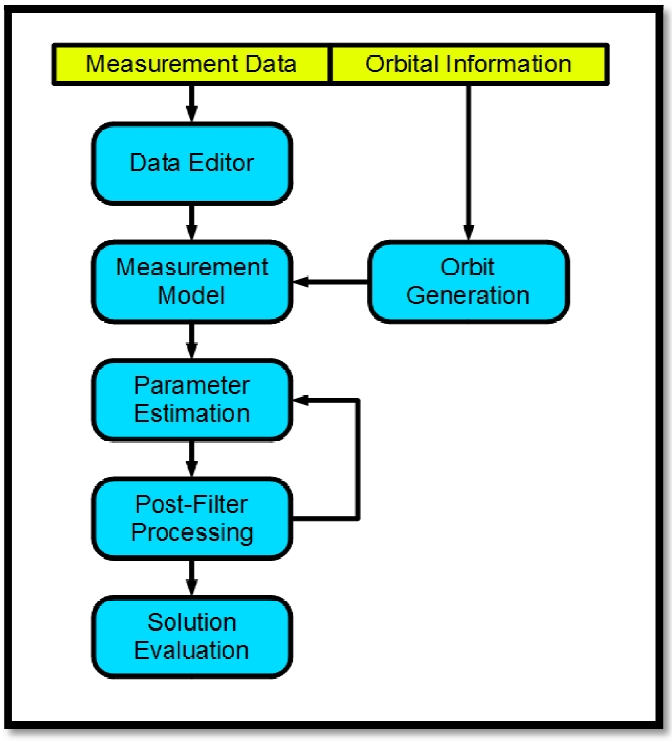

FIGURE 3. A TYPICAL GIPSY-OASIS DATA FLOW (JET PROPULSION LABORATORY, 2010)

Data consisting of satellite observations is collected in a RINEX file, which is the input to a program file called ninja. RINEX (Reciever Independent Exchange) files are, as the name suggests, independent of what receiver they are collected from. There are two kinds of RINEX files, namely single frequency and double frequency. Single frequency files hold only carrier wave data from L1 and code data from C1, while double frequency RINEX files consist of carrier wave data from both L1 and L2 as well as code data from both C1 and C2 (Gutner, 2002). The ninja program reads the RINEX files, reorders the data and writes the satellite data to individual binary fortran files, called quick measurement, qm, files. The individual qm files are then merged into a single file with the help of a program called merg_qm. Two scripts, qr_nml and s2nml, are used for creating a so called qregres namelist, suitable for the subsequent qregres program, from a merged qm file and other station information.

The other input data branch, containing satellite orbit data, begins with an orbit generator script called genoi. This script works with two namelists, tp.nml containing data of time along with polar motion and trajedy.nml containing satellite orbit data. The orbit generator module creates so called oi files consisting of satellite state data including position, velocity, acceleration and partials as a function of time. In the same way as several qm files were merged into one with the use of merg_qm, merge_sat is used in order to merge several oi files into one that can be added to the qregres namelist mentioned above. (Gregorius, 1996)

The qregres namelist is put into the qregres program, which interprets the namelist values and applies built-in physical models in order to create a regres file called rgfile, adjusted according to the models. The physical models hold correction terms concerned with measurement and Earth models, including tidal effects, phase centre offset, clock behavior and tropospheric effects, among many other (Gregorius, 1996). The output regres file is prepared for the following filtering process, starting with two steps of basic preparation for the actual filtering algorithm coming into play in a module simply called filter. The filtering algorithm is a modified Kalman filter called

Square Root Information Filter (SRIF), producing up to five optional output files with the final arrays along with smoothing coefficients, transition matrices and other parameters.

Subsequently, a function called smapper computes and maps the covariance, sensitivity and solution before post-fit data residuals are calculated by the postfit script. The output file, postfit.nio, carries both the pre- and post-fitted residuals. The postbreak command is then used for discovering discontinuities in the postfit.nio file. If previously passed on cycle slips are present the procedure is re-run with a modified qm file. If no cycle slips are found, however, outliers in the filtered output data are deleted with edtpnt2. After that step the smapper and postfit functions have to be re-run with the updated data files. The user can then evaluate the results and verify that no points need to be rejected. If modifications are needed the results are looped back to edtpnt2 for readjustment. If the results seem satisfying, however, they are passed on to the stacov software tools, which are used for creating readable text files. The ambigon2 script is an optional tool for adjusting the ambiguity resolution in order to obtain a more bias-free outcome. (Gregorius, 1996)

The stacov software tools, including the programs stacov, heightfix, stamrg, project, statistics and transform, interpret the smcov.nio file and, as previously mentioned, create readable output files. The output data is stored in so called stacov files, in ASCII format, to be interpreted and used directly or for further post-processing. (Gregorius, 1996)

2.2.2. GD2P.PL

As mentioned earlier, the GIPSY-OASIS software is under continuous development. An important step in the progress came in late 2008 with the new program gd2p.pl, short for GPS Data to Position. The program, written in the programming language Perl, works as a part of the traditional GIPSY-OASIS software and uses many of the already featured modules but, however, takes over the roles of others. gd2p.pl can be used for static and kinematic point positioning as well as precise orbit determination.

The outcome of running gd2p.pl is not only the final position solution, named tdp_final, but also three other important files. An executable script called run_again is created for running the program again, allowing the user to either keep the options used previously or make modifications. In addition, eventual errors are collected in gd2p.err while gd2p.log can provide a log of which GIPSY programs where executed and how. (Jet Propulsion Laboratory, 2008)

2.2.3. GPS NETWORK PROCESSOR

Over the past years new software has been developed at JPL for efficient processing of GPS ground station data from large networks. The software, called GPS Network Processor, runs with modules from GIPSY-OASIS using precise point positioning and bias fixing. In conformity with regular use of GIPSY-OASIS, the network processor has a command line interface where the user can decide what software features to use or not to use.

The GPS Network Processor software consists of three main programs, simply called a.pl, b.pl and c.pl. At start, the software expects a RINEX archive with station data at the local computer where the processing is to take place, from where files are copied to a directory called pp_input. The first main program, a.pl, moves input RINEX files from pp_input to another directory called pp_in_process, and initializes the script run_gd2p.pl, which point positions the RINEX files and places the results in a tree under the pp_output directory organized by year and day. The second program, b.pl, runs the script run_amb_day.pl for each day, either creating clusters of sites or keeping the sites separate, if desired, and then performing ambiguity resolution on each baseline. The results, ending up in a year and day of year tree under a directory called amb_output are then merged into one single stacov file in a directory called mrg_final for the user to view. The third program, c.pl, finally runs the script run_staproject.pl for each day. The script transforms the stacov file containing the final result to International Terrestrial Reference System (ITRF) coordinates and gets rid of the included covariance matrix. At last, the ultimate results are copied to an archive directory specified by the user. (Newport, 2006)

2.3. NOAA/NCEP ATMOSPHERIC PRESSURE DATA

National Centers for Environmental Prediction (NCEP) is part of the U.S. National Weather Service (NWS), which in its turn is governed by the National Oceanic and Atmospheric Administration (NOAA). NCEP provides national as well as international meteorological data and statistics used in many instances; governmental, corporative and private. (NOAA, 2007)

Global pressure field reanalysis data for the atmospheric loading data used in this project is provided by NCEP at the Computational and Information Systems Laboratory (CISL) Research Data Archive in 6-hourly data sets, collected each day at 0:00 UT, 6:00 UT, 12:00 UT and 18:00 UT, in a 2.5° x 2.5° grid.

2.4. INVERTED BAROMETER EFFECT

At sea the concept of an Inverted Barometer Effect, IBE, is often used for estimating elastic fluctuations of the sea level due to atmospheric loading. Moreover, IBE is not only present at sea but also comes into play over land. The effects, however, are not as large as they are at sea. By IBE is understood both vertical and horizontal movements of mass in connection to atmospheric pressure loading at ground surface. It bases on the trivial principles of pressure behavior, saying that elastic bodies deform and move their mass towards low-pressure environments. (Wunsch & Stammer, 1997)

The magnitude of the effect is most often expressed by the direction dependant ratios between the crustal response and the exerted atmospheric pressure. In the vertical direction the ratio is approximately 0.4 mm/hPa on land (approximately 10 mm/hPa at sea), but the figure is highly dependent on the properties of the underlying soil. Thus, sites located in the vicinity of a coastline or on an island will respond differently than inland sites to an equal magnitude of atmospheric pressure loading (van Dam, Blewitt, & Heflin, 1994). The sketch in Figure 4 below shows a two dimensional example of the Inverted Barometer Effect, IBE.

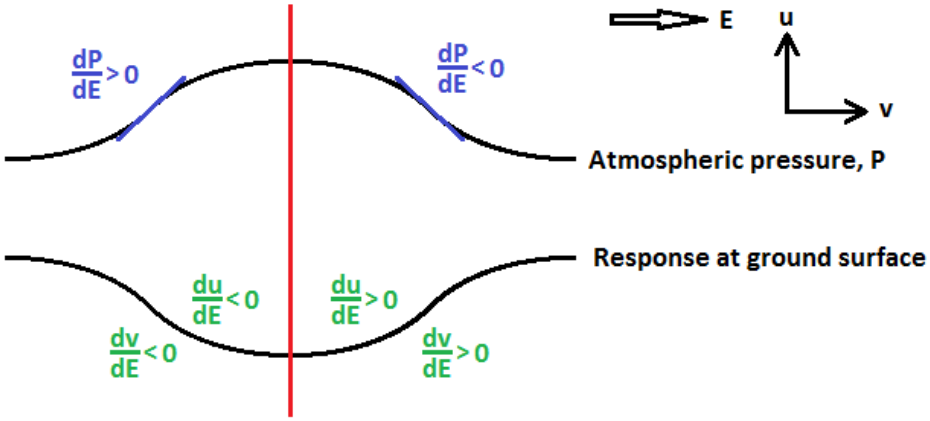

FIGURE 4. A TWO DIMENSIONAL EXAMPLE OF IBE

3. IMPLEMENTATION

The implementation part of this project can be divided into two different development processes. The first part comprises software development for collecting atmospheric pressure loading data in grids with appropriate resolution. The second part consists of developing new GIPSY interfaces for comprehensive modeling of east, north and vertical movements caused by atmospheric pressure loading. Moreover, the both parts need to be compatible with one another, thus contain data sets with agreeing units, formats and coordinate systems.

3.1. ACQUISITION OF GPS TIME SERIES DATA

The analysis is based on GPS tracking data collected using GIPSY-OASIS software, as previously described. Initially, GPS position data is processed for a period of time from May 1st 2009 through June 29th 2010 for a number of chosen stations with the GPS Network Processor. Subsequently a program called staseries is used for creating time series from the individual location data. The program staseries is, as most other GIPSY-related programs, based on a command line user interface, where a file containing the reference location of a certain station is declared followed by the other files to be combined in the time series and optional user preferences. Time series have to be created for each station individually using staseries.

Running staseries gives output in the form of three files for each station; one with latitude (*.lat), one with longitude (*.lon) and one containing radial component data (*.rad). An optional feature, which is used in this project, is to also include position residuals in the staseries results.

3.2. ACQUISITION OF ATMOSPHERIC PRESSURE LOADING DATA

For the implementation of atmospheric pressure loading in the analysis, atmospheric pressure loading time series are provided by the Goddard Very Long Baseline Interferometry (VLBI) group at NASA Goddard Space Flight Center; available on the Web at *http://gemini.gsfc.nasa.gov/aplo* (Petrov &

Boy, 2004). Below is described in short the method used for calculating atmospheric loading from atmospheric pressure data.

Reanalysis pressure data is, as previously mentioned, collected from NCEP at CISL Research Data Archive in 6-hourly data sets over a 2.5° x 2.5° grid. Moreover, the original data files contain ground or sea level pressure data, expressed in Pascal (Pa) along with longitude, latitude and geopotential height for each point in the grid. The model gives mean surface pressure and comprises a model of diurnal and semi-diurnal variations computed from NCEP reanalysis data over a period of time spanning from 1980 through 2002. (Petrov, Atmospheric Pressure Loading Service, 2008)

Using the pressure data, global distribution of atmospheric pressure loading is computed by Green's functions, presented in appendix B, in accordance with Farrell (1972) and bases on the Preliminary Reference Earth Model (PREM). PREM is an extensive data set containing a radial model of the Earth with numerous geophysical parameters, such as distribution of density and seismic velocities (Dziewonski & Anderson, 1981). The displacements derived from atmospheric pressure loading are calculated in relation to the center of mass of the solid Earth and the atmosphere combined. (Petrov, Atmospheric Pressure Loading Service, 2008)

In order to obtain an accurate and sufficiently precise model of the oceanic boundaries, the FES99 land-sea mask with 0.25° x 0.25° resolution was used. The oceanic response to atmospheric loading was then computed in accordance with the previously described inverted barometer effect theory (Petrov, Atmospheric Pressure Loading Service, 2008). The plots in **Figure 5** show amplitudes of the displacements caused by the diurnal (S_1) and semi-diurnal (S_2) variations in atmospheric loading according to the model.

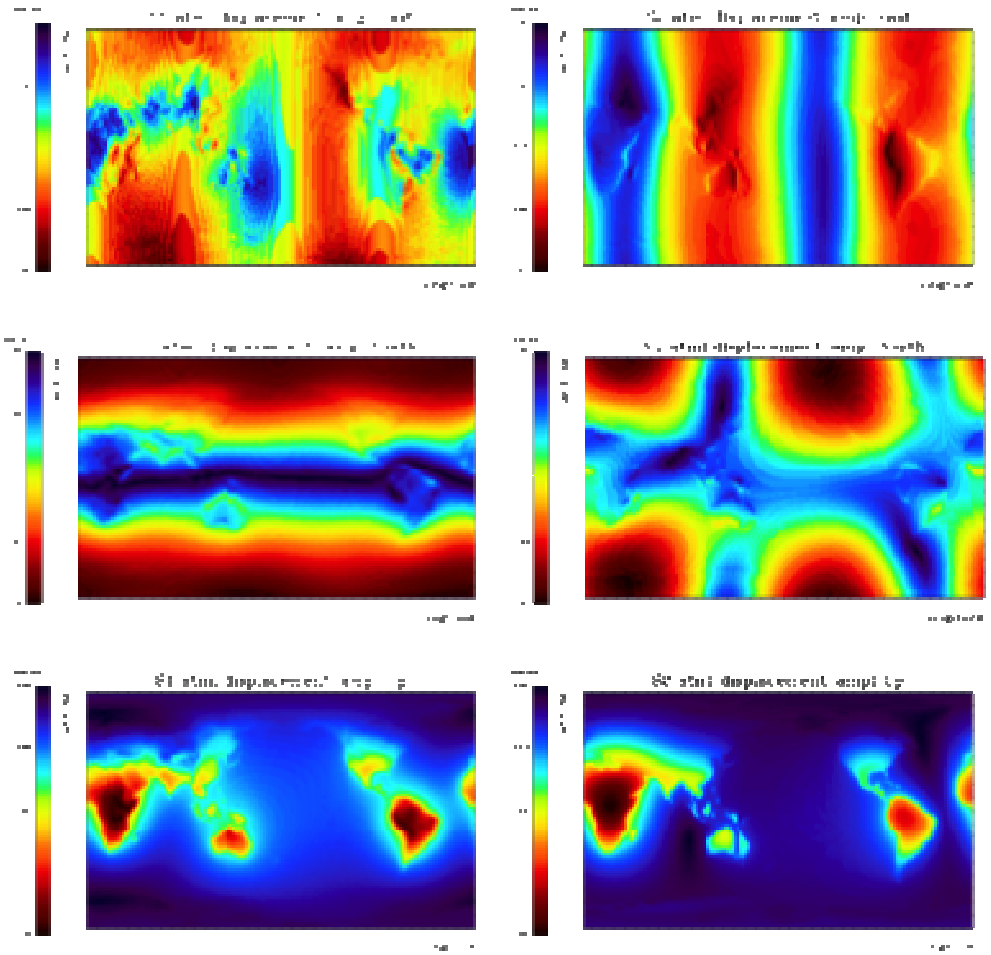

FIGURE 5. DISPLACEMENT CAUSED BY DIURNAL (S_1) AND SEMI-DIURNAL (S_2) VARIATIONS IN ATMOSPHERIC PRESSURE (PETROV, ATMOSPHERIC PRESSURE LOADING SERVICE, 2008)

As *van Dam, Altamimi, Collilieux and Ray* (2009) suggest, the rather coarse resolution of the reanalysis pressure data grid (2.5° x 2.5°) may be a cause for concern due to considerable topographic variation within grid cells. Since a large variation in topography typically gives large differences in atmospheric pressure, it may seem relevant to use a somewhat finer grid in mountainous regions. However, *van Dam, Altamimi, Collilieux and Ray* (2009) present two incentives for settling with the coarse grid. Firstly, their study indicates that less than 4 % of the grid points in the NCEP 2.5° x 2.5° grid show variations

greater than 200 m, when the effects have proven to be large enough to degrade results of GPS measurement. Secondly, as the topographic variation issue mainly matters in mountainous areas, where the ground in many cases consists of hard bedrock, the surface displacements will be very small. **Figure 6** below shows maximum topographic difference over a global 2.5° x 2.5° grid along with root-mean-square (RMS) variability of elevation.

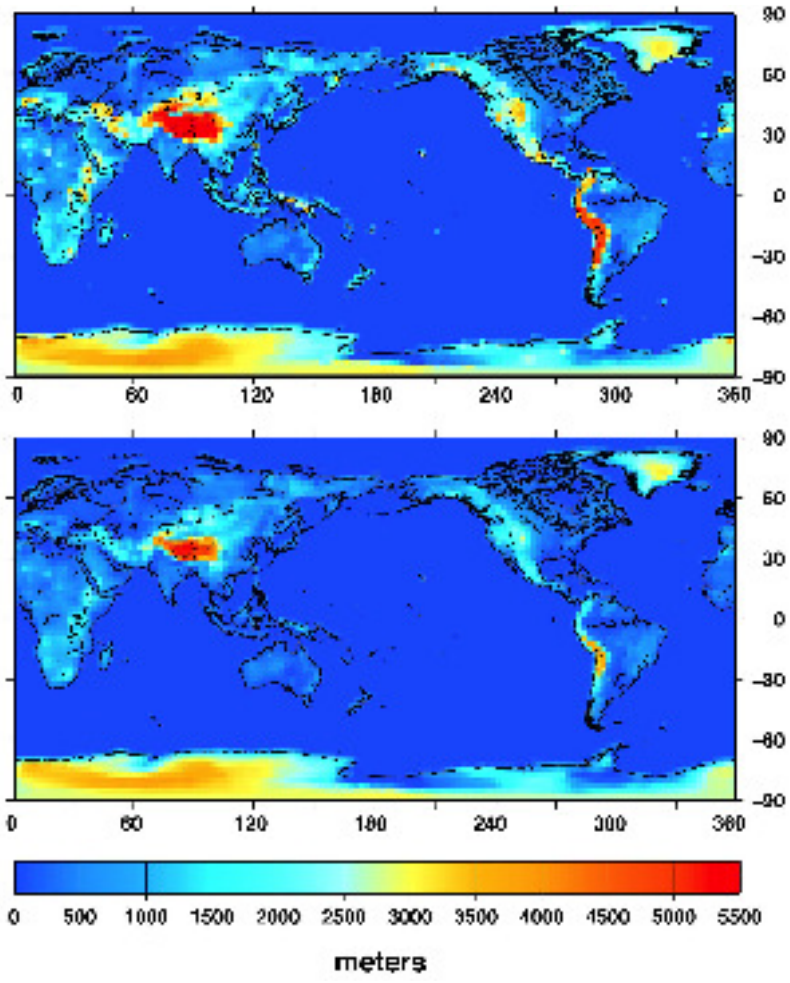

FIGURE 6. UPPER: MAXIMUM TOPOGRAPHIC DIFFERENCE OVER A 2.5°X2.5° GRID. LOWER: RMS VARIABILITY OF ELEVATION OVER A 2.5°X2.5° GRID. (VAN DAM, ALTAMIMI, COLLILIEUX, & RAY, 2009)

3.3. Applying Atmospheric Pressure Loading to Time Series Data

When finally combining the two preceding steps, the displacement vectors caused by atmospheric pressure loading is subtracted from the original time series data, according to the principle commonly referred to as o – c (or omc), meaning observed data minus computed data. This principle is generally used in GPS processing when correcting observational data.

For this particular project, a program was written in Perl programming language to read observed and computed data in order to subtract the displacements caused by the atmospheric pressure loading. The program outputs time series data in the same format as the original, non-corrected, time series data in order to facilitate use of the corrected data and comparison between the two. Before applying the model on the time series data, daily averages where created from the provided 6-hourly atmospheric pressure loading data, in order to decrease the influence from diurnal and semi-diurnal variation.

4. MODEL VERIFICATION

Throughout the implementation process GPS site data has been used for testing processing software and analyzing the results. Below is described the approach for testing and verifying the accuracy of the implementation model.

4.1. SITE SELECTION

All stations used in the project belong to the IGS tracking network and are considered to provide consistent and reliable data for the analysis. Apart from this, the choice of stations is also based on location. In order to obtain a broad variety of data with all types of variations in atmospheric loading the selected sites are spread globally.

For the analysis, all used stations are also situated at least 500 km from the nearest ocean coastline in order to avoid interference from ocean loading and tidal effects. The total number of stations used is 29, which is considered to be large enough to provide reliable results but still small enough for the processing to be performed within a reasonable amount of time. Below, **Figure 7** displays a map showing the locations of all sites used in the analysis whilst a complete list of the stations is shown in

Table 1.

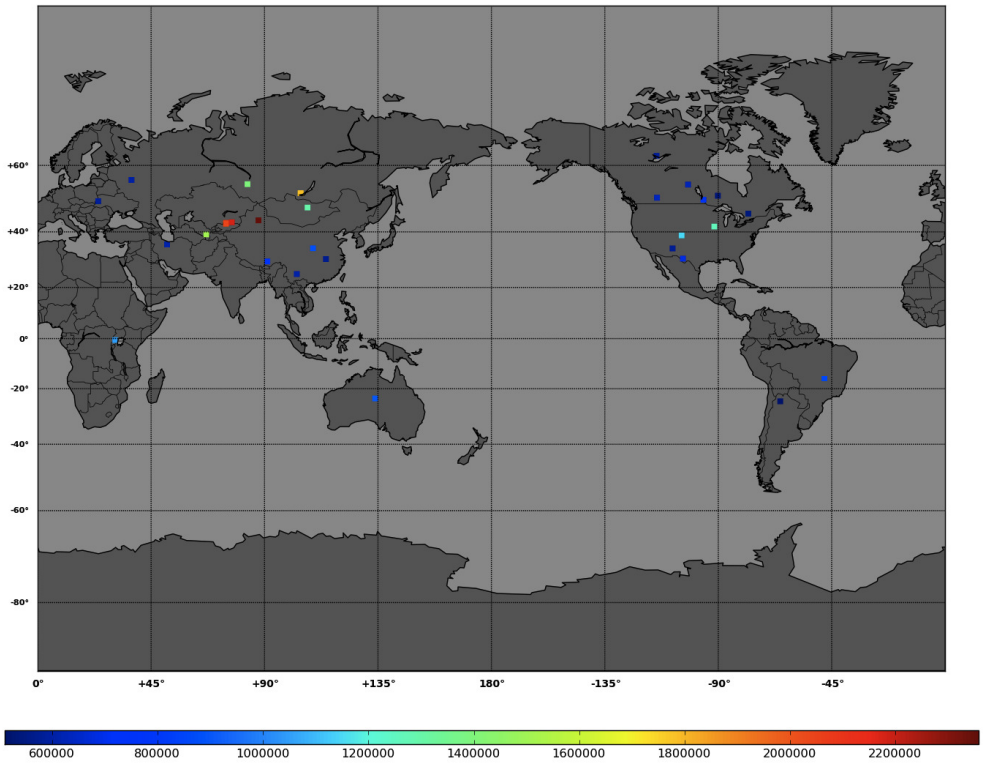

FIGURE 7. THE COLORED DOTS REPRESENT THE 29 STATIONS USED IN THE ANALYSIS. THE COLORS INDICATE DISTANCE TO NEAREST OCEAN ACCORDING TO THE SCALE AT THE BOTTOM. NOTE THAT ALL STATIONS ARE SITUATED AT LEAST 500 KM FROM THE NEAREST OCEAN SHORE.

TABLE 1. THE 29 STATIONS USED IN THE ANALYSIS

Station ID	No.	Location	Country	Lon (E)	Lat (N)	Altitude (m)	Dist. to coast (m)
ALGO	1	Algonquin Park	Canada	281,9286	45,9588	201,4	538431
ALIC	2	Alice Springs	Australia	133,8855	-23,6701	603,7	899809
AMC2	3	Colorado Springs	U.S.A.	255,4754	38,8031	1912,5	1149910
BRAZ	4	Brasilia	Brazil	312,1222	-15,9474	1106,0	860715
CHUM	5	Chumysh	Kazakhstan	74,7511	42,9985	716,3	2077430
DUBO	6	Lac Du Bonnet	Canada	264,1338	50,2588	251,0	773545
FLIN	7	CFS Flin Flon	Canada	258,0220	54,7256	320,0	627010
IRKJ	8	Irkutsk	Russia	104,3162	52,2190	502,1	1785250
KIT3	9	Kitab	Uzbekistan	66,8800	39,1400	643,0	1505810
KUNM	10	Kunming	China	102,7972	25,0295	1986,2	607385
LHAZ	11	Lhasa	China	91,1040	29,6573	3622,0	766567
MBAR	12	Mbarara	Uganda	30,7379	-0,6015	1337,7	1047310
MDO1	13	Fort Davis	U.S.A.	255,9850	30,6805	2004,5	689398
MDVJ	14	Mendeleevo	Russia	37,2145	56,0215	257,4	596298
NLIB	15	North Liberty	U.S.A.	268,4251	41,7716	207,1	1266130
NVSK	16	Novosibirsk	Russia	83,2355	54,8406	123,6	1399710
PICL	17	Pickle Lake	Canada	269,8380	51,4798	315,1	533360
PIE1	18	Pie Town	U.S.A.	251,8811	34,3015	2347,7	579328
POL2	19	Bishkek	Kyrgyzstan	74,6943	42,6798	1714,2	2043210
PRDS	20	Calgary	Canada	245,7065	50,8713	1247,0	632610
SELE	21	Almaty	Kazakhstan	77,0168	43,1791	1340,0	2178380
SULP	22	Lviv	Ukraine	24,0145	49,8356	370,5	584023
TEHN	23	Tehran	Iran	51,3341	35,6973	1194,6	615699
ULAB	24	Ulaanbataar	Mongolia	107,0500	47,67	1611,7	1299190
UNSA	25	Salta	Argentina	294,5924	-24,7275	1257,8	509277
URUM	26	Urumqi	China	87,6300	43,59	856,1	2357430
WUHN	27	Wuhan City	China	114,3573	30,5317	25,8	568800
XIAN	28	Lintong	China	109,2215	34,3687	81,6	882602
YELL	29	Yellowknife	Canada	245,5193	62,4809	181,0	583112

An alternative approach towards avoiding ocean loading intervention could be to base the choice of stations on the size of the ocean loading coefficients at each station, i.e. use stations with ocean loading coefficients less than a certain threshold value. This approach, however, was not used because of the fact that ocean loading coefficients have daily variation. As in this project daily average values are used for calculating atmospheric pressure loading, the daily variation in ocean loading may bring that ocean loading is applicable at certain stations at some points in time although the coefficients fall below the threshold in average over the day.

Moreover, no considerations concerning properties of the underlying rock or soil structures at the stations are taken into account in the project. It is likely that this affects the loading behavior, but as the pressure grid is rather coarse

(2.5° x 2.5°) the variation within each bin area is too great to model comprehensibly.

4.2. REPEATABILITY ANALYSIS

In order to analyze the accuracy of the results, time series are created by combining stacov files for each individual site, both with and without having applied correction terms for atmospheric pressure loading. As previously mentioned, the time series span from May 1st 2009 through June 29th 2010. The resulting time series, which are created using the program staseries, include site coordinates, repeatability about the initial reference position and residuals.

4.3. SCATTER ANALYSIS

The quality of the displacement data can be assessed by comparing the daily scatter within the time series before and after having applied terms of atmospheric loading. This is done by comparing standard deviation and variance for each time series. A reduction in scatter, thus reduction of standard deviation and variance, indicates a superior solution. Before performing the scatter analysis, outliers with values farther from the sample mean than three times the standard deviation are eliminated from the time series displacement data.

Prior to the scatter analysis the time series data is also prepared by subtracting the sample mean and removing eventual obvious trends within the data sets. Trends are removed by subtracting the equation of a line, fitted to the curve of the original data, from the displacement time series data. In order to reduce influence from annual behavior, a sine curve is fitted to each time series and subsequently subtracted. This procedure gives bias-free time series data with reduced power from linear and annual trends for the analysis.

In **Figure 8** below, plot A (top left) shows the original time series in red with the mean value in black. Plot B (top right) shows the same time series after

subtracting the mean in green and a fitted linear regression in black. Plot C (bottom left) shows the time series after subtracting the linear regression in blue and a fitted sine curve in black whilst plot D (bottom right) shows the final time series, prepared for further analysis.

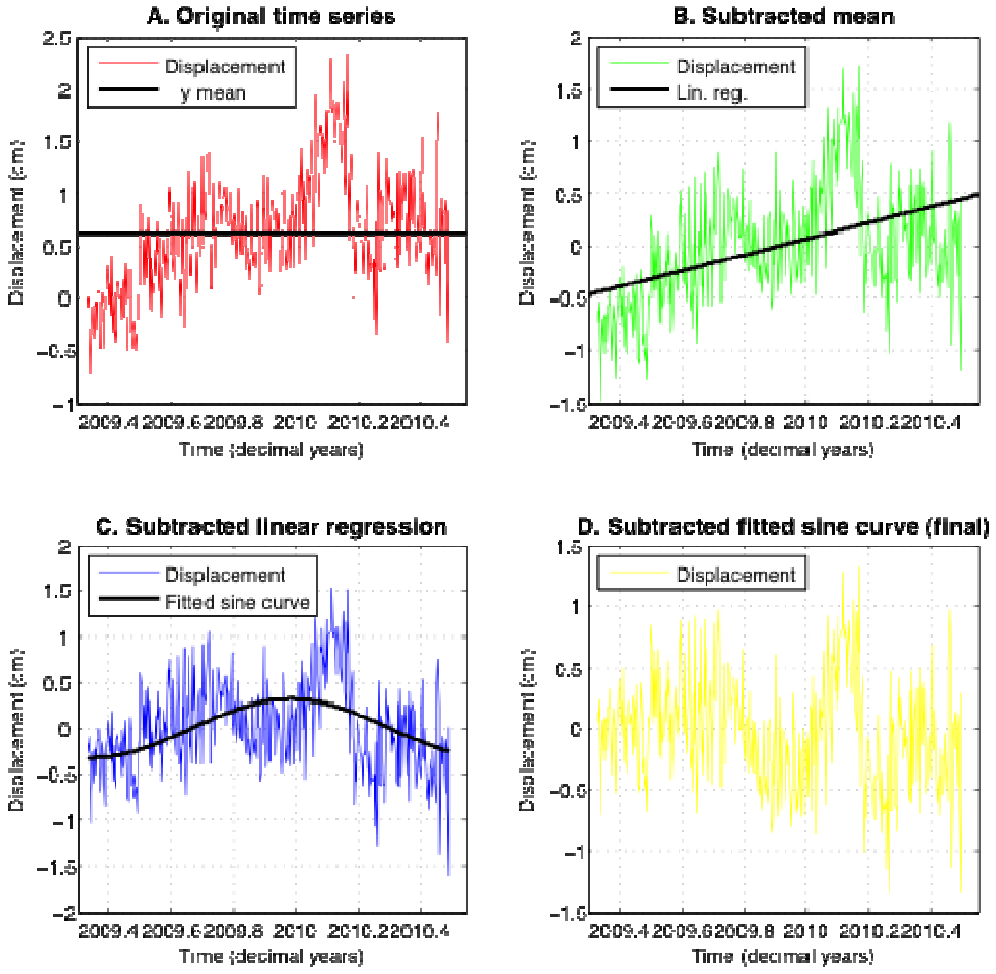

FIGURE 8. AN EXAMPLE OF THE PROCEDURE OF PREPARING TIME SERIES DATA FOR ANALYSIS, TAKEN FROM THE STATION IN YELLOWKNIFE (YELL)

4.4. SPECTRAL ANALYSIS

The periodogram is a tool for investigating periodic tendencies within time series data spectra. In this project it is used for finding relations between power and frequency as well as amplitude and frequency, respectively, among

the time series data. As for the scatter analysis, described above, outliers are eliminated before performing spectral analysis and linear trends are removed as well as annual tendencies. The program pdgram, written in Perl, then computes Fourier transformation and smoothes the periodogram results in order to provide comprehensible output data.

5. RESULTS

The results of the model verification, described in the previous chapter, imply that a higher degree of accuracy can be obtained by implementing atmospheric pressure loading in high precision GPS measurement. Below, the results from each step of the model verification process are presented.

5.1. ATMOSPHERIC PRESSURE LOADING EFFECTS

According to above, time series are created with and without applying the model of atmospheric pressure loading effects. **Figure 9** shows an example of time series for Bishkek, Kyrgyzstan in latitudinal, longitudinal and radial directions, respectively. The red lines represent the case where no atmospheric pressure loading model is applied and the green lines represent the case with having applied the model.

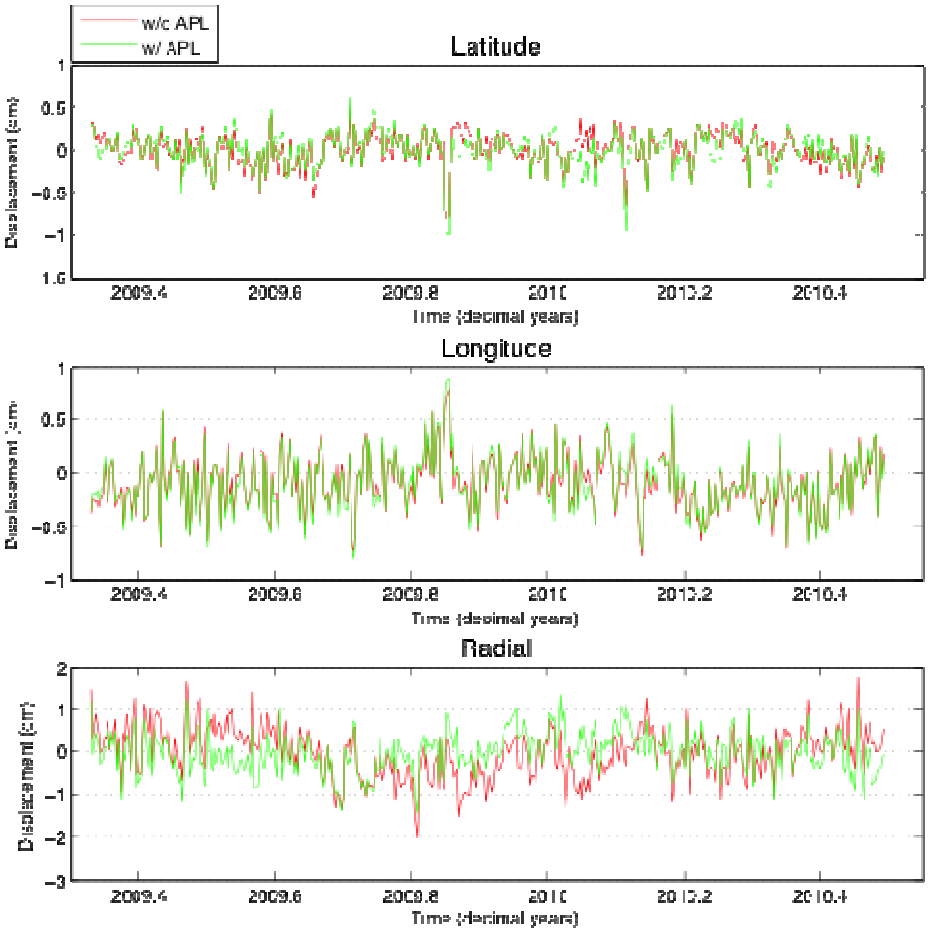

FIGURE 9. DISPLACEMENT TIME SERIES FOR BISHKEK (POL2)

Comparing the differences in displacement after applying the model for atmospheric pressure loading to the original time series gives the direct effects of the model, and thus the loading, assuming the model is correct. An example of this, again for Bishkek, is shown in **Figure 10**. The plots show that the model has the most impact on the vertical component, where estimates at this site vary from -1.67 cm to 0.86 cm. Atmospheric pressure loading causes displacement of 0.42 cm at maximum at Bishkek during the investigated period of time in the latitudinal direction and half as much, 0.21 cm, longitudinally.

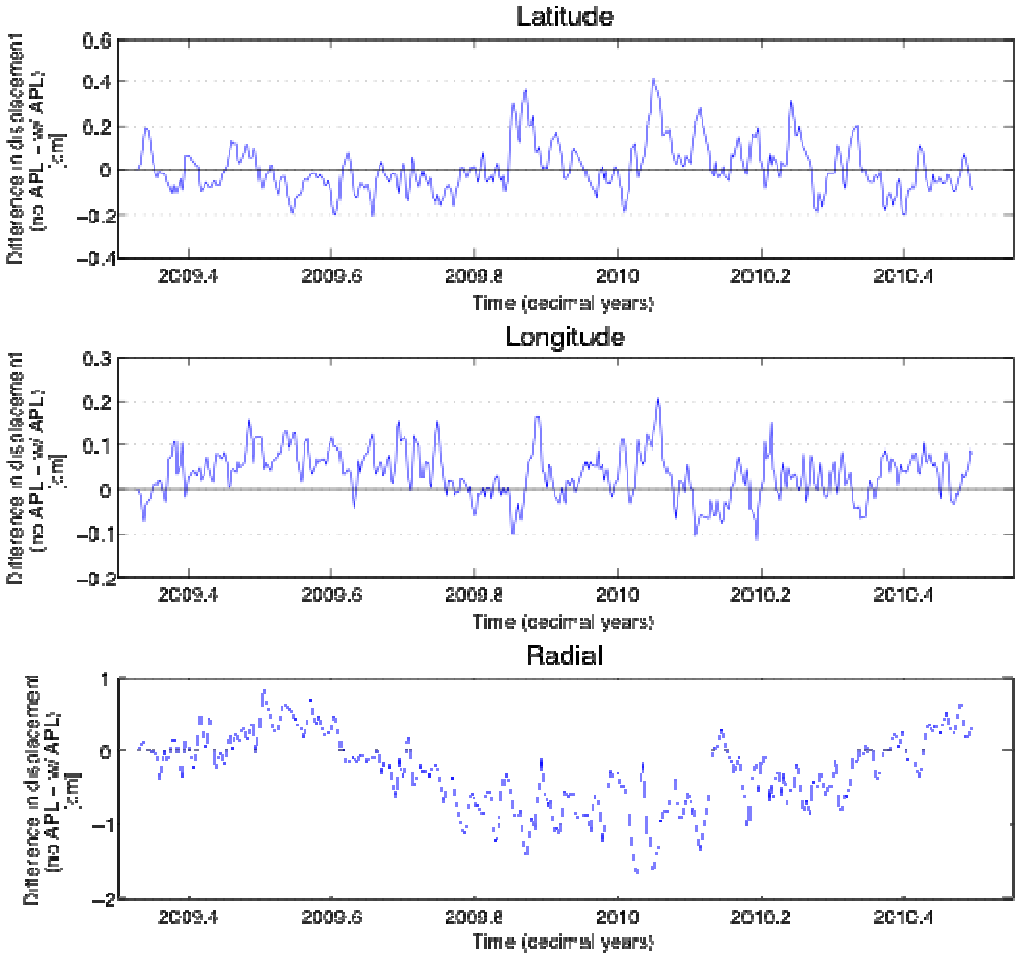

FIGURE 10. DIFFERENCES IN DISPLACEMENT TIME SERIES AT BISHKEK (POL2) WITH AND WITHOUT APPLYING THE MODEL FOR ATMOSPHERIC PRESSURE LOADING

The plots in **Figure 11**, showing averages (red circles) of suggested displacement caused by atmospheric pressure loading at each station and standard deviation (blue bars), indicate that it is not only at Bishkek the largest impact is seen in the radial direction, but for all other stations included in the analysis as well. Furthermore, most results show the least impact from the model in the longitudinal direction whilst the latitude is affected slightly more. The displacements in the radial direction, however, are significantly larger. Note that plotted means are absolute values and the signs (positive or negative) only determine the directions of displacement.

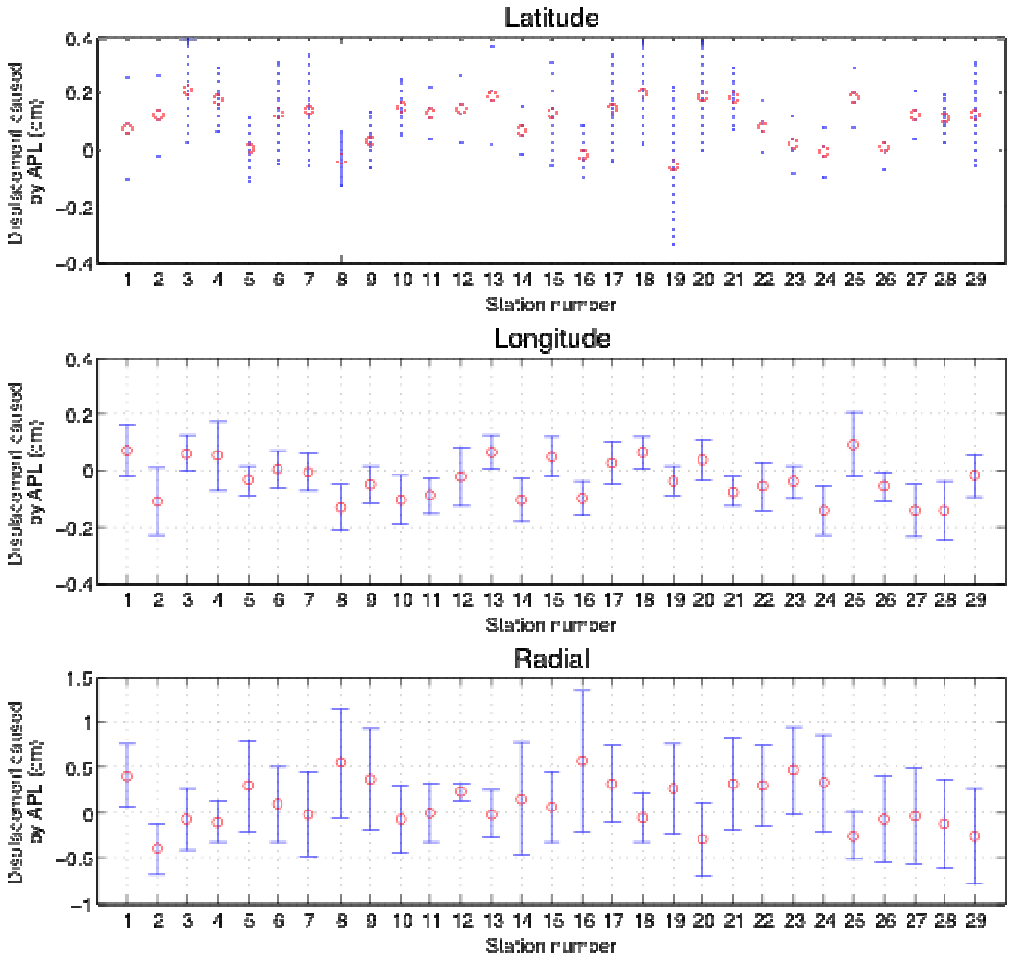

Figure 11. The red circles represent mean displacement caused by Atmospheric pressure loading at each station. The blue bars show standard deviation. Stations are numbered according to

TABLE 1.

Looking at maximum displacement caused by atmospheric pressure loading it is, again, obvious that the largest movements are found in the vertical direction.

Typically, maximum values for longitudinal displacement are less than 5 mm while they in average are 5 mm for the latitude and 15 mm for the radial, reaching as high as 32 mm at one point at the station in Novosibirsk, Russia (NVSK). The maximum displacements due to the modeled atmospheric pressure loading are shown as red circles in **Figure 12** with standard deviations represented by blue bars. Again, note that maximums are absolute values and the signs only show the directions of displacement.

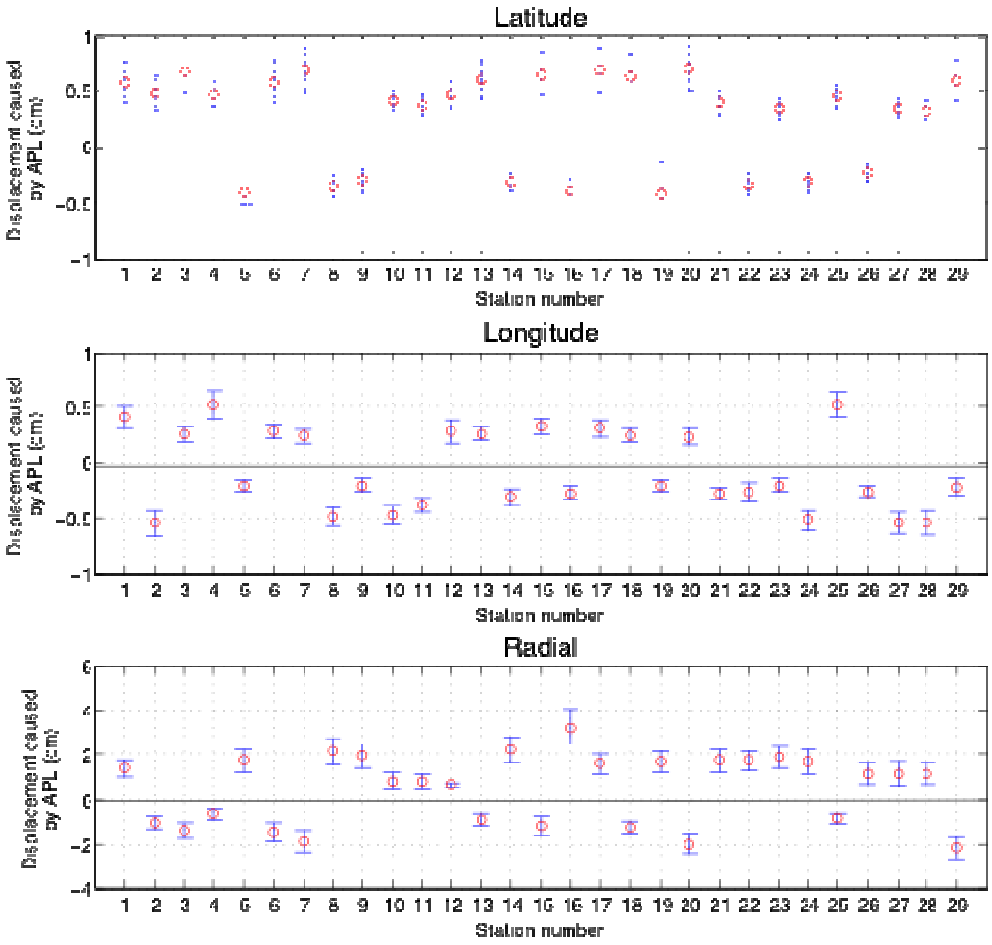

Figure 12. The red circles represent maximum displacement caused by Atmospheric pressure loading at each station. The blue bars show standard deviation. Stations are numbered according to

TABLE 1.

5.2. SCATTER ANALYSIS

Results of the scatter analysis show that a reduction of the data scatter within the time series can be obtained by implementing atmospheric pressure loading. As expected, the largest differences are found in the radial direction. However, the results are not entirely univocal.

5.2.1. STANDARD DEVIATION

Analysis of reduction in standard deviation when applying atmospheric pressure loading shows that the scatter in the longitudinal direction is almost not affected at all (in average the standard deviation increased by 0.0004 cm), whilst standard deviation reductions of up to 0.2657 cm can be found in the radial direction where a reduction of standard deviation appears at 26 of the 29 stations. Changes of insignificant magnitudes can be noticed in the latitude, where the standard deviation in average is increased by 0.0092 cm when applying atmospheric pressure loading.

The plot in **Figure 13** below shows the reduction of standard deviation for each station. In general, changes of standard deviation for the latitudinal and longitudinal time series data are rather small compared to those in the radial direction. Outliers are found at Colorado Springs, USA (station 3) for the latitude and at Kunming, China (station 10) for the radial component, showing relatively large increases in standard deviation as opposed to the expected reductions. Excluding these, a reduction of standard deviation is found at 93 % of the investigated sites for the radial and 59 % for the longitudinal component. However, in the latitude the standard deviation is reduced at only 25 % of the stations.

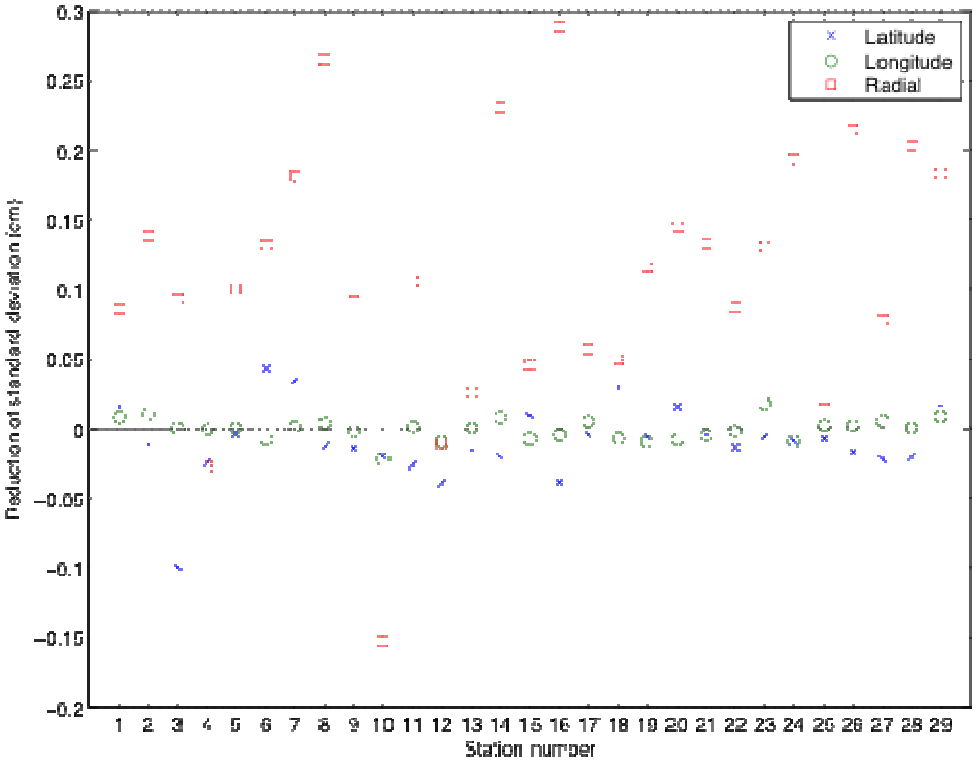

Figure 13. Reduction of standard deviation with Station numbers according to

TABLE 1.

5.2.2. VARIANCE

Since the magnitude of displacement varies significantly between different stations within the analysis it is important not only to investigate the scatter reduction in terms of absolute figures, but also as percentual reduction of an initial value. A convenient way of doing this is by looking at variance.

Figure 14, showing percentual reduction of variance for each of the investigated sites, reveals that rather large percentual changes in variance are present in the radial and latitudinal directions while only small changes are seen in the longitude. At the most, the radial component variance is reduced by 61 % (in Irkutsk, Russia). Excluding the outlier found in Colorado Springs, USA, the maximum percentual change in variance for the latitude is an increase of 28 %, found in Lhasa, China.

In average, variance is reduced by 28 % for the radial direction, while it was increased by 6 % (if excluding the outlier at the station in Colorado Springs) for the latitude. The longitude was as good as unaffected.

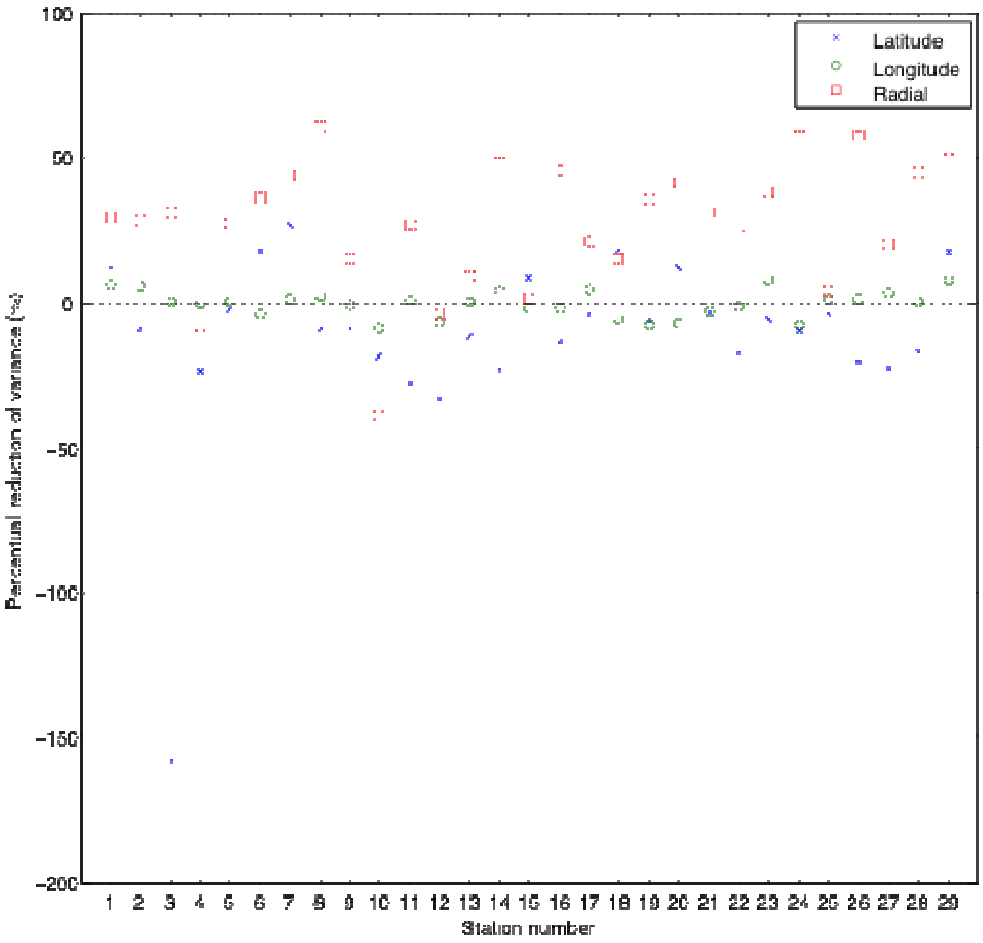

Figure 14. Percentual reduction of variance with station numbers according to

TABLE 1.

5.2.3. POSSIBLE CORRELATIONS

As described earlier, the magnitude of atmospheric pressure and thus atmospheric pressure loading is highly dependant on altitude. Accordingly, the meteorological data must be precise enough to give correct values of atmospheric pressure and the model for calculating and interpolating the derived loading to the specific sites must be precise enough to model the loading distribution correctly.

If the model would fail to describe the loading, trends may appear as results of correlation between altitude and measured displacement. However, plotting reduction of standard deviation against the altitudes at which the stations are located, as displayed in **Figure 15**, suggests that no such correlation exists at the sites included in this project.

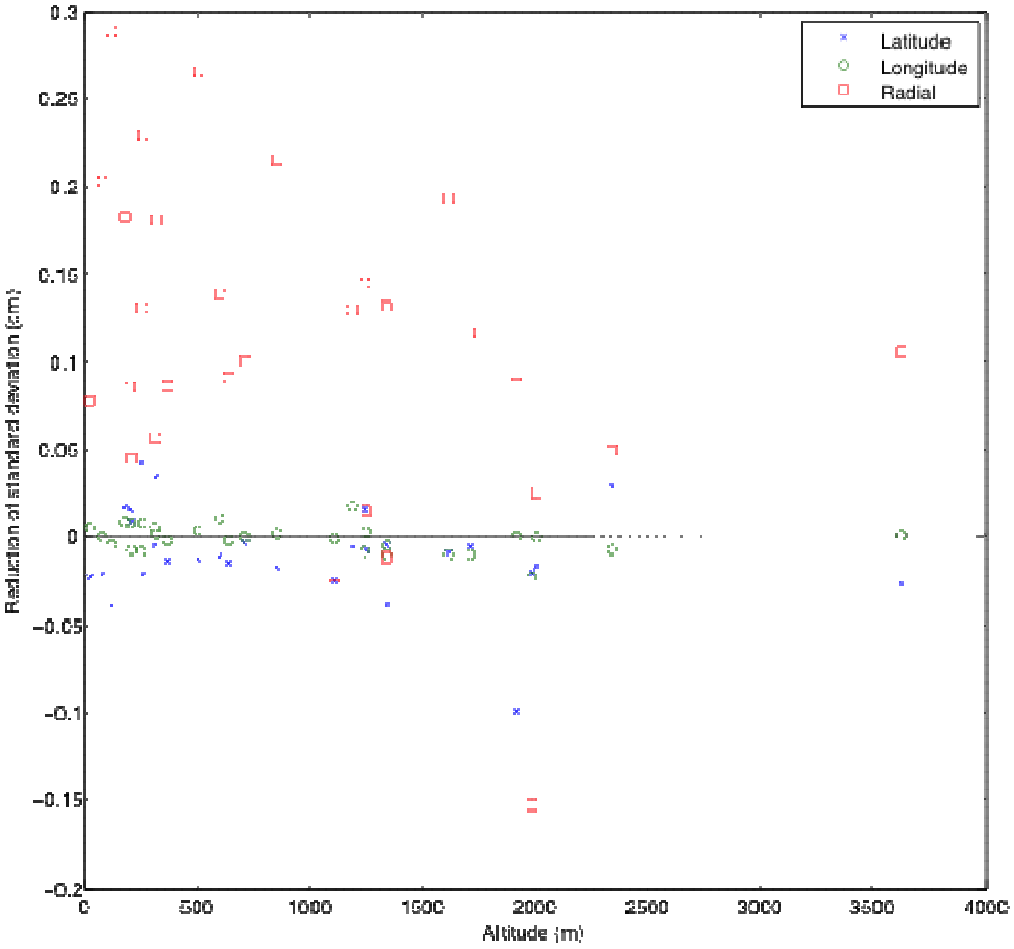

FIGURE 15. REDUCTION OF STANDARD DEVIATION PLOTTED AGAINST ALTITUDE

In the same way as for altitude, effects related to the distance to nearest shoreline may interfere with displacement data. If the model of atmospheric pressure loading fails to account for differences between oceanic behavior and the loading response over land, the results may be affected and thus carry unwanted biases.

The results from plotting reduction of standard deviation against distance to nearest ocean, as seen in **Figure 16**, are however not as easily interpreted as the plot with standard deviation against altitude. The reason for this is that the stations included in the analysis are all chosen because they are situated at a great distance from nearest shoreline. Thus, the plot does not necessarily

suggest that there is no correlation between the results and the distance to coast, although no signs of such a correlation can be found, but rather that all stations are situated sufficiently far from the closest ocean to be affected by it.

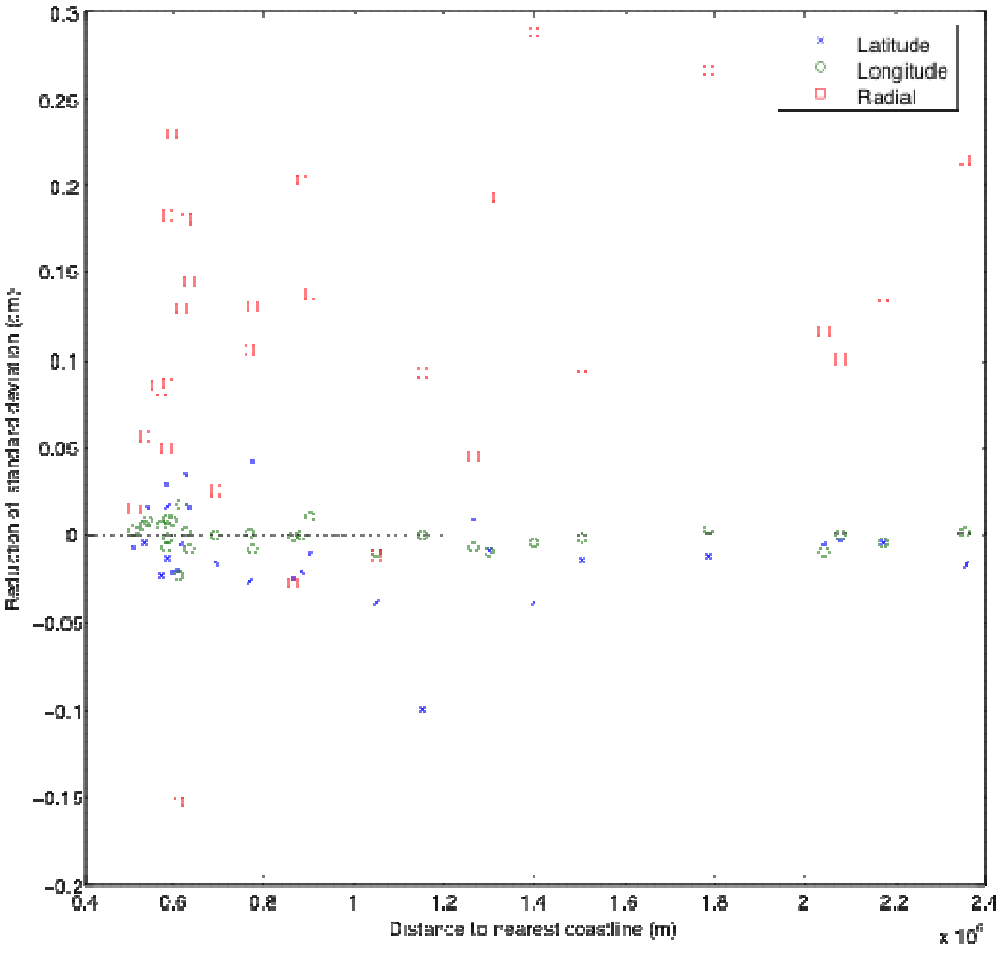

FIGURE 16. REDUCTION OF STANDARD DEVIATION PLOTTED AGAINST DISTANCE TO NEAREST COASTLINE.

5.3. SPECTRAL ANALYSIS

Before implementing the atmospheric pressure loading model, time series data was dominated by an annual power and as frequency increased, larger amounts of noise affected the signal. At many sites an additional peak can be found for the semi-annual frequencies in the power spectra. By applying the model, the annual peak is reduced at most stations but only small

improvements can be found in the high frequency noise. The semi-annual peaks are reduced to some extent, but generally not as much as the annual.

As the statistical scatter analysis above showed, the largest alterations between before and after applying the model of atmospheric pressure loading are found in the radial direction. Therefore, the spectral analysis is focused mainly on vertical displacement data. Periodograms of signals in the latitudinal and longitudinal directions, however, typically show the same effect as in the radial only with smaller differences between the two cases; with and without applied atmospheric pressure loading, respectively.

Figure 17 shows a log-scale periodogram of radial time series data from Irkutsk, Russia. The red line represents the case where no model of atmospheric pressure loading is applied, and the green line represents the case after implementing the model. Power reductions are found at most frequencies throughout the spectra, with the largest improvements at low frequencies. At frequencies around ~2.75 cycles per year energy is added to the signal, but the increase is not significant.

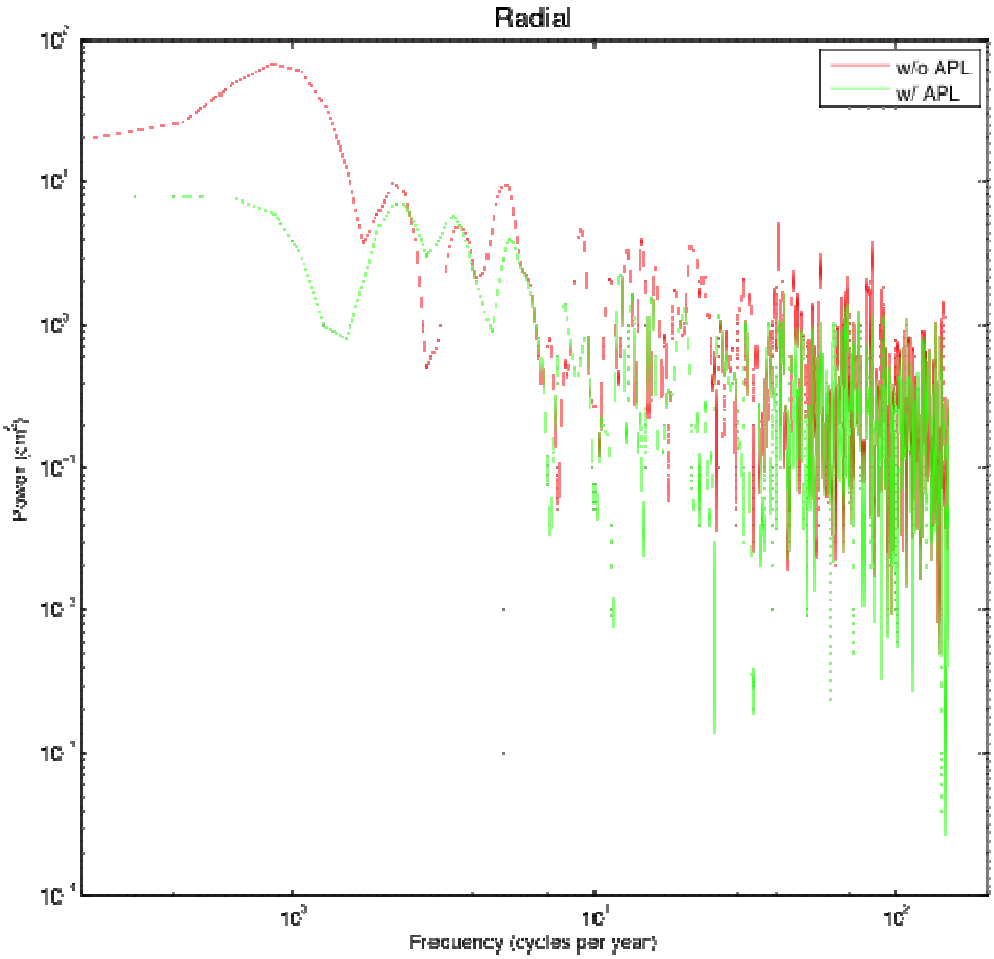

FIGURE 17. POWER SPECTRA OF RADIAL TIME SERIES DATA FROM IRKUTSK (IRKJ), RUSSIA

Another example of power spectra is given in **Figure 18**, showing a periodogram of radial time series data from Lac du Bonnet, Canada. Again, the red line represents the case without atmospheric pressure loading and the green line corresponds to the case with the model applied. At this station a larger resemblance between the two cases is seen at low frequencies, whilst the largest reductions in the power spectra are found in frequencies from 2 to 20 cycles per year (with the exception around 4.5 cycles per year, where power is added). This implies a different behavior than the example above, from Irkutsk. Assumingly the meteorological conditions are causing the

dissimilarities. The high frequency noise is still present for both cases at Lac du Bonnet as at the Irkutsk station data.

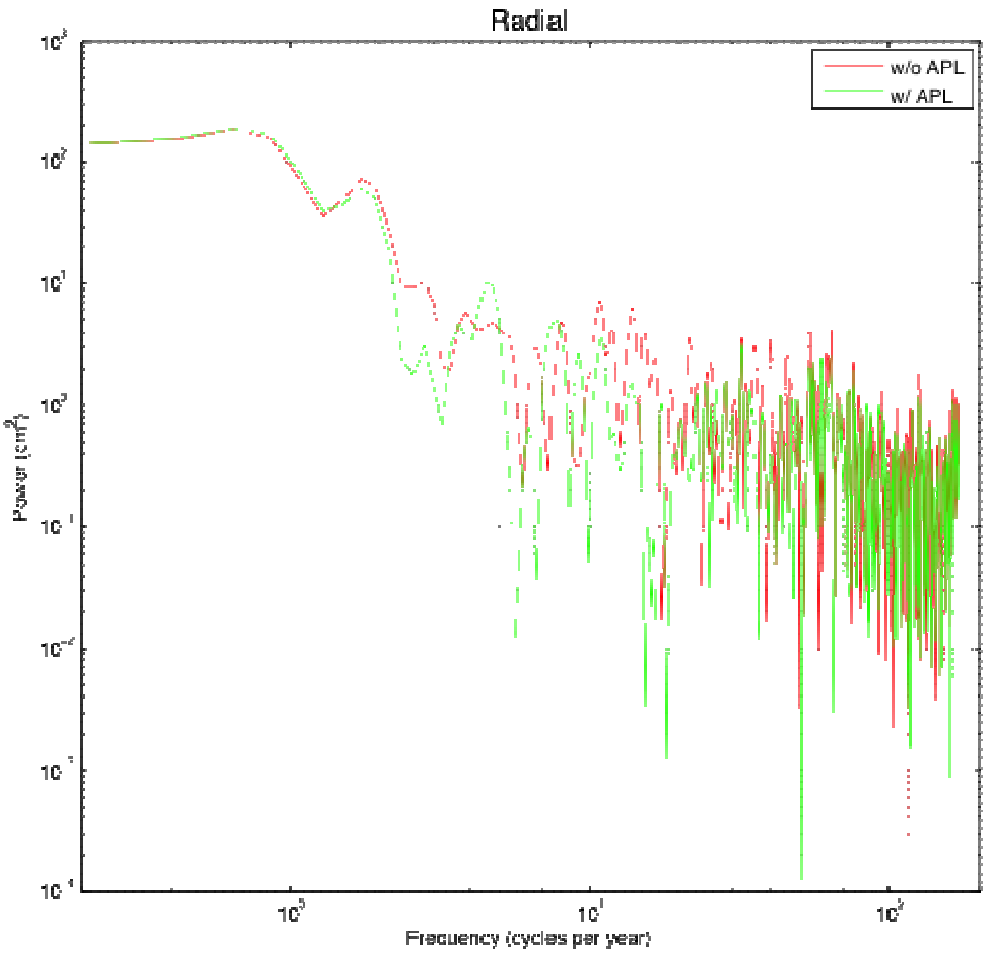

FIGURE 18. POWER SPECTRA OF RADIAL TIME SERIES DATA FROM LAC DU BONNET (DUBO), CANADA

Another way of analyzing periodicity and secular variation within time series data is to use periodograms with amplitude on the y-axis instead of power. Such plots basically show the same things as does the ones displaying power, which is nothing but the amplitude squared. However, they can be easier to interpret as amplitude, given in cm, is more applicable in the analysis.

Figure 19 below shows the amplitude periodogram of vertical displacement time series data from Irkutsk, Russia. The red line symbolizes the case with no atmospheric pressure loading model and the green line represent the case with the model applied. As for the power periodogram for the same station, shown previously in **Figure 17**, the improvement around the annual (frequencies around 1 cycle per year) is evident, as is the insignificant degradation at frequencies somewhat lower than 3.

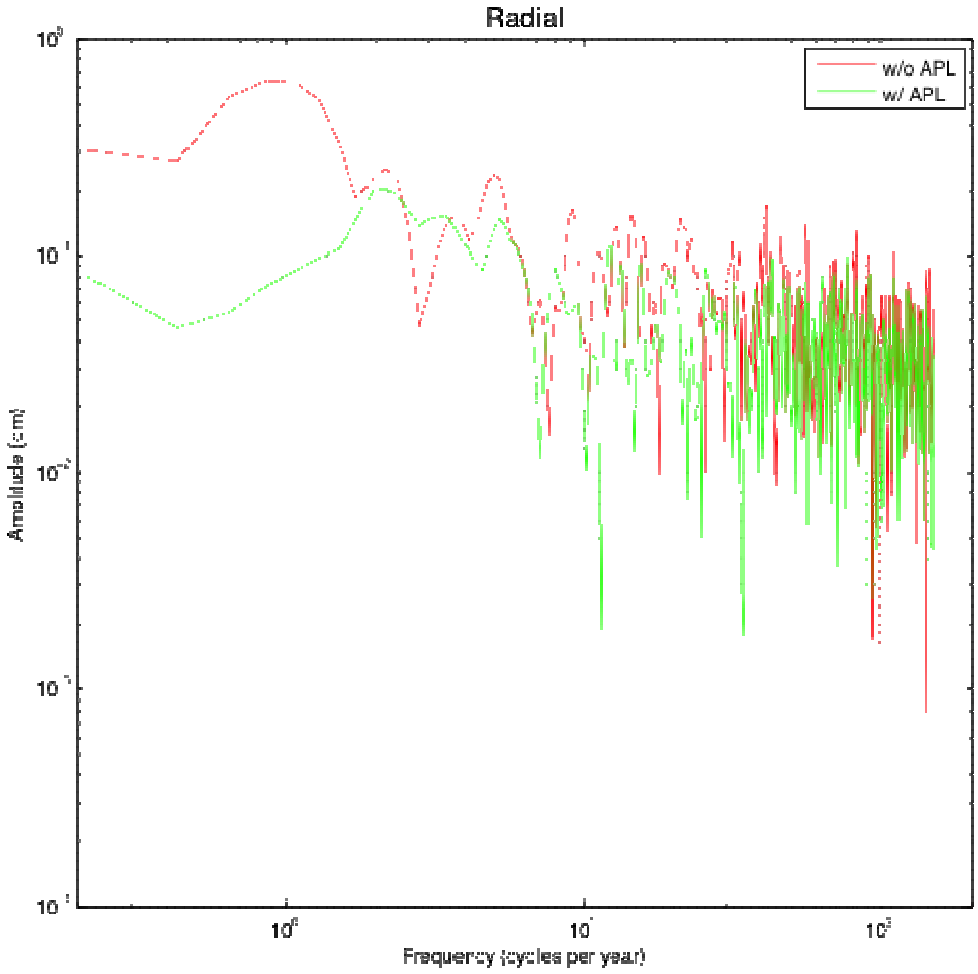

FIGURE 19. AMPLITUDE PERIODOGRAM OF RADIAL TIME SERIES DATA FROM IRKUTSK (IRKJ), RUSSIA

Obvious similarities between power and amplitude periodograms can also be seen in **Figure 20** if compared to what was previously presented in **Figure**

18. The red line continuously represents the case without atmospheric pressure loading whilst the green line represents the situation when the model is implemented.

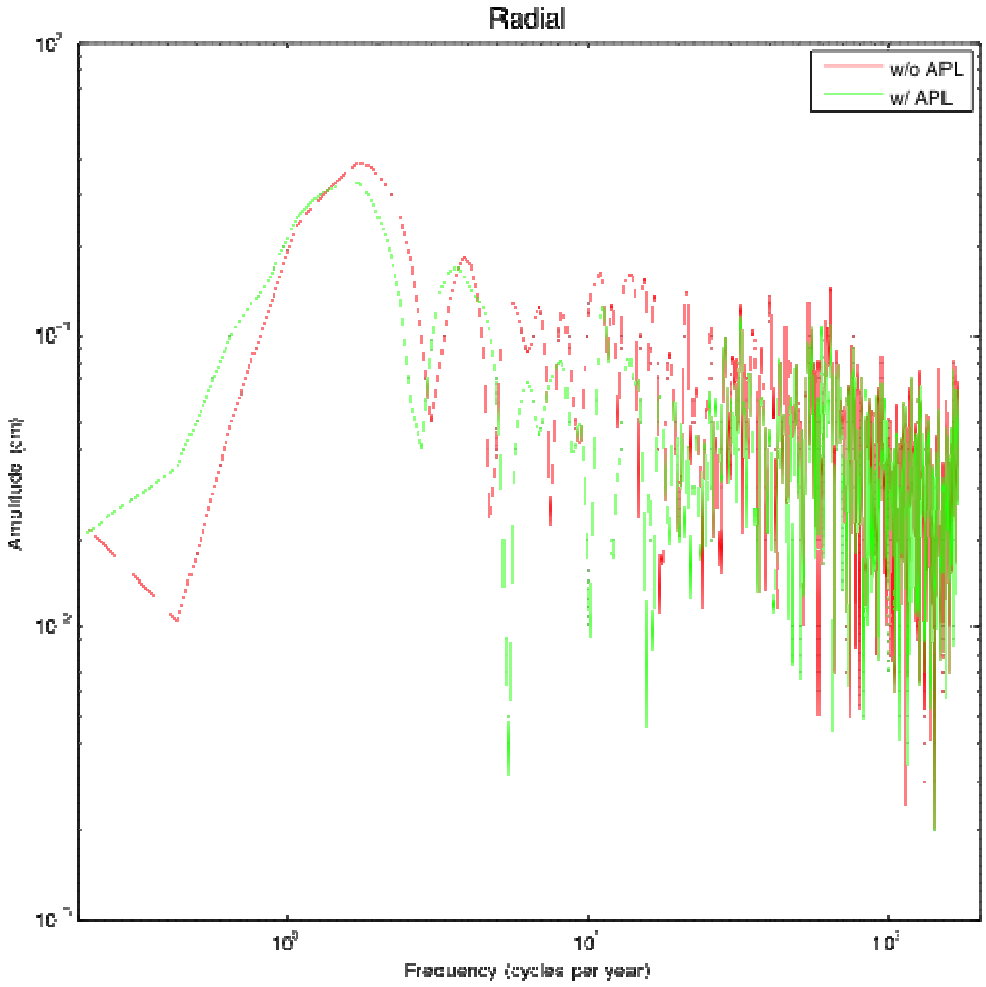

FIGURE 20. AMPLITUDE PERIODOGRAM OF RADIAL TIME SERIES DATA FROM LAC DU BONNET (DUBO), CANADA

6. DISCUSSION

The results show reason to believe that implementing the model of atmospheric pressure loading will improve the precision of GPS measurement, especially affecting the vertical component of position vectors. Nevertheless, there are remaining issues causing noise to interfere with the measurement data, which may result in deficiencies within the analysis. Such issues can be divided into three main categories. Firstly, the procedure of the analysis itself may contain shortcomings. Secondly, the model of atmospheric pressure loading may be slightly inaccurate and, thirdly, other phenomena may affect the GPS measurement time series data.

Regarding the analysis, the main issues are most probably associated with the quite limited number of stations used and the stations' locations, along with the fact that daily averages where used for the analysis instead of the original 6-hourly displacement data. All included stations are situated far (>500 km) from the oceans where the effect of atmospheric pressure loading is likely to be at its greatest.

As a next step in this process of implementing atmospheric pressure loading in GIPSY-OASIS, it is suggested to include more stations in the test-runs. Furthermore, the stations are to be situated closer to the ocean in order to examine influence from ocean loading. Subsequently, the 6-hourly displacement data can be used instead of the daily averages to enable analysis of short-term fluctuations such as tidal effects. The procedure of the analysis, however, is considered to be consistent and reliable.

The main source of potential disadvantages in this project is the model for calculating atmospheric pressure loading from meteorological pressure data. First and foremost, the pressure data provided by NCEP may be inaccurate. As the global distribution of meteorological stations, at which pressure data is collected, is uneven with more dense coverage of North America and western Europe than the rest of the world, the pressure fields created from the measured data may be inadequate.

Furthermore, the pressure grid is rather coarse (2.5 ° x 2.5 °), which can lead to insufficiently modeled pressure distributions at some sites, especially in areas

with lots of local variations for example in mountainous regions. Neither is the grid fine enough to account for variations of the rock or soil structures underlying the GPS stations. A station located on soft clay is more likely to be affected by atmospheric pressure loading than is a station situated on extensive igneous rock.

It is possible that the Green's functions used in the model for computing loading distribution from atmospheric surface pressure contain inadequacies. Assessments found in literature solely compare the specific functions used in this project to other Green's functions, arguing only that the used Green's functions are better than their "rival" in the assessments. It does not, in fact, prove that the fundamental physical assumptions, on which all Green's functions are based, are accurate. It is possible that the effects of atmospheric pressure loading are, in some cases, overestimated by the model.

Another difficulty in connection to this project is the fact that atmospheric pressure loading is not the only phenomena bringing noise to GPS measurement data. Also other signals, which may interfere with the atmospheric loading effects, are present. How well a certain effect is modeled is hard to tell, especially if other phenomena interfere destructively and the effects add each other out. If that is the case, applying a model of only one of the effects could cause more harm than benefit.

Moreover, other phenomena than atmospheric pressure loading are causing crustal deflections. For example, variations in water storage at lakes and in the underlying soil have proven to result in movements on the surface of the Earth. Such effects can be both random and follow trends, as precipitation and water storage volume generally is seasonally dependant. Some stations included in the analysis are situated in the vicinity of seas and lakes of considerable sizes and may thus be subject to such effects.

7. CONCLUSIONS

Crustal movements caused by variations in atmospheric pressure are found to affect the accuracy of high precision GPS measurement. By applying a model of the deflections, it is possible to reduce the effects and thus enhance the accuracy. In this Master of Science thesis, an evaluation of the effects from applying such a model is presented.

The model uses NCEP (National Centers for Environmental Prediction) reanalysis pressure data to calculate crustal movements by convolving Green's functions according to Farrell (1972). Pressure data is collected at 6-hourly intervals over a 2.5° x 2.5° grid. Displacement time series are created from high precision GPS measurements at 29 GPS stations located more than 500 km inland. The model of atmospheric pressure loading is applied on the time series in terms of daily average values, derived from the 6-hourly data, in order to avoid influence from diurnal and semi-diurnal variations. Subsequently, the two sets of time series; the original data without the model (1), and after having applied the model (2), where analyzed by comparing data scatter and periodicity.

Results of the analysis show that measurement data scatter can be reduced by implementing the model. The largest reductions are found in the radial direction, whilst generally only insignificant effects are found in the longitude. Statistical analysis shows that data scatter in the latitudinal direction is somewhat degraded, but the effects are very small compared to those in the radial. In average, the variance within the time series data scatter was reduced by ~28 % for the vertical component, increased by ~6% for the latitude and unaffected (~0 % change) for the longitude.

Spectral analysis with periodogram indicate that for most stations, the largest benefits from applying the model for atmospheric pressure loading are found at low (around annual) frequencies. At some stations, however, the most significant reductions are found at mid-frequencies, proving that local environment determines the nature of the loading response.

In conclusion, results show positive effects of implementing the atmospheric pressure loading model. However, further analysis is needed before including

the model in GIPSY-OASIS GPS data processing procedure. As a next step, it is recommended that more stations are included, situated closer to the oceans in order to investigate how well the oceanic response is modeled. Furthermore, the original 6-hourly data is suggested to be included instead of daily averages, to enable sub-daily variation.

8. REFERENCES

Dziewonski, A. M., & Anderson, D. L. (1981). Preliminary reference Earth model. *Physics of The Earth and Planetery Interiors , 25* (4), 297 - 356.

Farrell, W. E. (1972). Deformation of the Earth by Surface Loads. *Reviews of Geophysics and Space Physics , 10* (3), 761 - 797.

Gregorius, T. (1996). *GIPSY-OASIS II: How it works...* Newcastle: Department of Geomatics, University of Newcastle upon Tyne.

Gutner, W. (2002 йил 25-01). *SWEPOS.* Retrieved 2010 йил 17-05 from RINEX: The Receiver Independent Exchange Format Version 2.10: http://swepos.lmv.lm.se/rinex/rinex210.txt

IGS Central Bureau. (2007 йил 26-07). *IGS Central Guidelines*. Retrieved 2010 йил 01-06 from International GNSS Service: http://igscb.jpl.nasa.gov/network/guidelines/guidelines.html#allsites

Jet Propulsion Laboratory. (2008). Introduction to gd2p.pl. *GIPSY User Group Meeting/Class.* Pasadena, CA: JPL.

Jet Propulsion Laboratory. (2010). *Introduction to GIPSY Software.* Pasadena, CA: California Institute of Technology.

Newport, B. (2006). *User's Guide GPS Network Processor Version 3.0.* Pasadena: Jet Propulsion Laboratory.

NOAA. (2007 йил 23-08). *About NCEP*. Retrieved 2010 йил 12-07 from National Centers for Environmental Prediction: http://www.ncep.noaa.gov/about/

Petrov, L. (2008 йил 01-11). *Atmospheric Pressure Loading Service*. Retrieved 2010 йил 19-07 from The Goddard Geodetic VLBI Group's Gemini auxiliary web pages: http://gemini.gsfc.nasa.gov/aplo/

Petrov, L., & Boy, J.-P. (2004). Study of the atmospheric pressure loading signal in very long baseline interferometry observations. *Journal of Geophysical Research , 109*.

Seeber, G. (1993). *Satellite geodesy : foundations, methods, and applications.* Berlin ; New York: Walter de Gruyter & Co.

U.S. National Executive Committee for Space-Based Positioning, Navigation and Timing. (2009 йил 28th-May). *The Global Positioning System*. Retrieved 2010 йил 5th-May from Space-Based Positioning, Navigation & Timing: http://www.gps.gov/

van Dam, T. M., Blewitt, G., & Heflin, M. B. (1994). Atmospheric pressure loading effects on Global Positioning System coordinate determinations. *Journal of Geophysical Research , 99* (23), 939 - 950.

van Dam, T., Altamimi, Z., Collilieux, X., & Ray, J. (2009). *Topographically Induced Height Errors in Predicted Atmospheric Loading Effects.* Faculte des Sciences de la Technologie et de la Communication. Luxembourg: University of Luxembourg.

Wells, D., Beck, N., Delikaraoglou, D., Kleusberg, A., Krakiwsky, E. J., Lachapelle, G., et al. (1986). *Guide to GPS Positioning.* Fredericton, N.B., Canada: Canadian GPS Associated.

Wunsch, C., & Stammer, D. (1997). Atmospheric Loading and the oceanic "Inverted Barometer" Effect. *Reviews of Geophysics , 35*, 117 - 135.

APPENDIX A

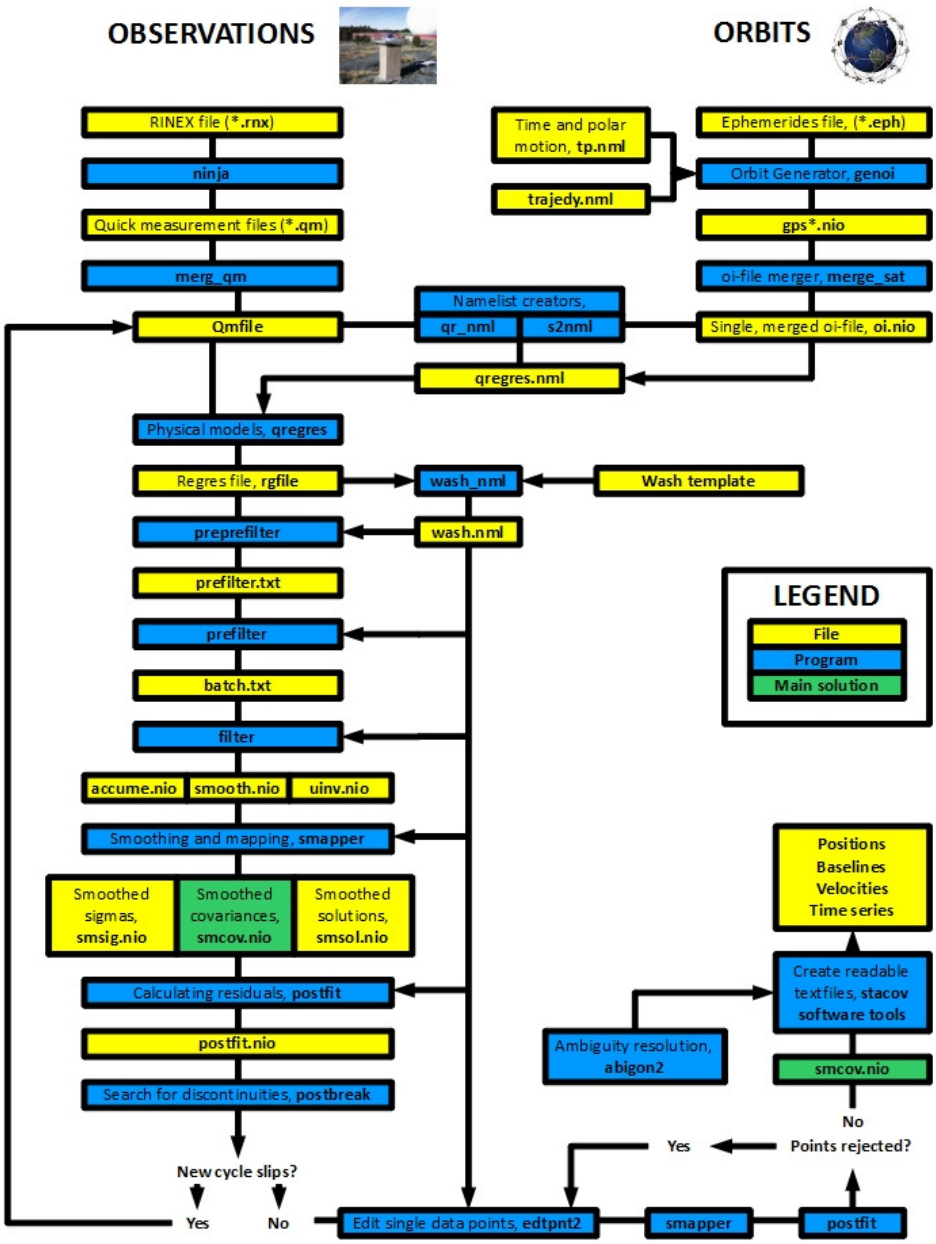
OBSERVATIONS
ORBITS
RINEX file (*.rnx)
ninja
Quick measurement files (*.qm)
merg_qm
Qmfile
Time and polar motion, tp.nml
trajedy.nml
Ephemerides file, (*.eph)
Orbit Generator, genoi
gps*.nio
oi-file merger, merge_sat
Namelist creators,
qr_nml
s2nml
Single, merged oi-file, oi.nio
qregres.nml
Physical models, qregres
Regres file, rgfile
wash_nml
Wash template
preprefilter
wash.nml
prefilter.txt
prefilter
batch.txt
filter
accume.nio
smooth.nio
uinv.nio
Smoothing and mapping, smapper
Smoothed sigmas, smsig.nio
Smoothed covariances, smcov.nio
Smoothed solutions, smsol.nio
Calculating residuals, postfit
postfit.nio
Search for discontinuities, postbreak
New cycle slips?
Yes
No
Edit single data points, edtpnt2
smapper
postfit
Points rejected?
Yes
No
Ambiguity resolution, abigon2
Create readable textfiles, stacov software tools
smcov.nio
Positions
Baselines
Velocities
Time series
LEGEND
File
Program
Main solution

APPENDIX B

Vertical displacements, u_r, are computed with the following formulae, according to Farrell (1972) and Petrov and Boy (2004):

$$u_r(r,t) = \iint \Delta P(r',t) G_R(\psi) \cos\varphi' \, d\lambda' \, d\varphi'$$

where, r is the site coordinates
t is the time
ΔP is the variation in surface pressure
GR is the vertical Green's function (see below)
ψ is the angular distance between the station with coordinates r and the pressure source with coordinates r'
φ' is the geocentric latitude and
λ' is the longitude

The vertical Green's function is:

$$G_R(\psi) = \frac{fa}{g_0^2} \sum_{n=0}^{+\infty} h'_n \, P_n(\cos\psi)$$

where, f is the universal constant of gravitation (as defined in PREM)
a is the Earth's radius (as defined in PREM)
g_0 is the mean surface gravity (as defined in PREM)
h_n' is a computed Love number and
P_n is the Legendre polynomial of degree n

Horizontal displacements, u_h, are computed with the following formulae:

$$u_h(r,t) = \iint q(r,r') \Delta P(r',t) G_H(\psi) \cos\varphi' \, d\lambda' \, d\varphi'$$

where, q(r,r') is the unit vector originating from the station, tangential to the Earth's surface and
G_H is the tangential Green's function (see below)

$$G_H(\psi) = -\frac{fa}{g_0^2}\sum_{n=1}^{+\infty} l'_n \frac{\partial P_n(\cos\psi)}{\partial\psi}$$

where, l'_n is a computed Love number